https://doi.org/10.26599/FRICT.2026.9441225

Research Article

Friction behaviors in incremental sheet forming with rolling and sliding friction

Guangcan Yang, Dawei Zhang*, Chong Tian, Shengdun Zhao

School of Mechanical Engineering, Xi'an Jiaotong University, Xi'an 710049, China

* Corresponding author: Dawei ZHANG, E-mail: zhangdawei2000@mail.xjtu.edu.cn

Received: March 13, 2024; Revised: August 13, 2025; Accepted: January 26, 2026

Abstract: The tribological mechanisms governing microstructure evolution in incremental sheet forming (ISF) were investigated through comparative analysis of three friction modes: sliding friction (ISF-SF), rolling friction (ISF-RF), and frictionless free-deformation (ISF-FD). Systematic characterization of interfacial interactions, grain refinement mechanisms, and texture evolution demonstrated that friction-induced shear deformation served as the dominant factor in determining forming performance. Crucially, ISF-RF preserved {110} texture integrity via nondirectional shear deformation, where effective lubrication suppressed interfacial plowing, adhesion, and oxidation, thereby achieving superior surface finish and minimal twist angle in formed parts. Conversely, ISF-SF drove directional shear deformation that actively reoriented grains toward {001} texture. Reduced lubrication efficacy intensified texture strength while amplifying interfacial plowing, adhesion, oxidation, and crack propagation, ultimately increasing part twist angle. The study elucidated the mechanism by which friction governs forming performance through shear deformation: moderate deformation coupled with grain refinement enhanced formability, whereas excessive deformation led to detrimental effects, including stress concentration, interface defects, and oxidation-accelerated failure. These findings establish a microstructure-property-process relationship, advancing ISF technology towards texture-regulated friction mode selection and adaptive lubrication strategies that balance grain refinement and defect suppression. This theoretical foundation enables next-generation ISF systems with enhanced forming limits and tailorable material properties.

Keywords: incremental sheet forming; rolling friction; sliding friction; friction behaviors

Nomenclature

F_d	Material deformation resistance	R	Tool radius
F_x	Forming force in *x*-axis	t	Sheet thickness
F_y	Forming force in *y*-axis	v	Feed speed
F_{xy}	Horizontal forming force	w	Spindle rotation speed
F_z	Forming force in *z*-axis	Z	layer-downward displacement
f	Friction force	α	Wall inclination angle
ISF	Incremental sheet forming	α_{max}	Maximum forming angle
ISF-FD	Incremental sheet forming with frictionless free-deformation	μ	Friction coefficient
ISF-RF	Incremental sheet forming with rolling friction	σ_t	Normal stress
ISF-SF	Incremental sheet forming with sliding friction	β	Part twist angle
S	Deformation contact area	GND	Geometrically necessary dislocation

KAM	Kernel Average Misorientation	HAGBs	High-Angle Grain Boundaries

1 Introduction

Incremental sheet forming (ISF) offers enhanced formability [1] and improved process flexibility [2] through localized deformation [3, 4]. Friction significantly influences the accuracy of shape [5], surface quality [6], and the force required for forming [7] in this process. A deep understanding of friction behaviors provides a scientific foundation for choosing the most appropriate lubrication methods and materials for specific conditions, thereby maximizing benefits and minimizing friction's adverse effects, thus enhancing forming performance and production efficiency. Currently, research on the friction aspects of the process mainly focuses on how different friction conditions affect surface finish [8]. In-depth studies on friction behaviors are scarce, highlighting the need for further research to uncover frictional interactions in the ISF process, especially those coupled with plastic deformation.

Friction is a key factor influencing the ISF process. In ISF experiments on AA5052-H32, Xu et al. [9] revealed that excessive shear effects from pure sliding friction could precipitate premature material failure. A transition to combined rolling and sliding friction modes reduces friction and consequently enhances formability. Echoing this, Strano et al. [10] found that increased friction forces diminish formability, a conclusion supported by Jeswiet et al. [11] and Kim and Park [12]. The study by Silva et al. [13] on forming hole-flanges using single point incremental forming (SPIF) demonstrated that the interaction between the forming tool and the sheet metal resulted in plastic flow and fracture. Contrarily, studies suggest that lower friction forces result in minimal through-thickness shear effects, which are beneficial for formability [14, 15]. Emmens et al. [16] observed that shear stress lowers tensile yield stress, thereby stabilizing forming processes and significantly improving formability, especially by increasing the limiting draw ratio. Thus, diminished formability is linked to decreased thickness shear forces, reflecting reduced negative friction [17, 18]. Through a twist analysis model, Yang et al. [19] and Chang et al. [20] proposed that friction-induced shear effects twist the sheet metal geometry, potentially causing early material fracture, as argued by Carrino et al. [21]. Durante et al.

[22], in ISF experiments using spherical and hemispherical tools on AA7075-T0, showed that less friction smoothens surface roughness and lowers forming forces. Beyond affecting surface quality and formability, substantial friction in ISF impacts tool wear and material selection. Tools, often made from materials like high-speed steel (HSS) and hard alloys [23], are hardened or coated (e.g., TiN, CrN) [24] to enhance durability. It is evident that the friction effects during the ISF process directly impact formability, surface quality, and tool wear. Therefore, a deep understanding of the friction behavior in this process provides a new perspective to reveal the mechanisms behind changes in ISF formability and surface quality from a tribological standpoint.

Scholars have sought solutions to mitigate the adverse effects of friction on ISF surface quality by exploring different lubrication methods and friction modes. Lubricants create a thin oil film to prevent direct tool-to-sheet contact, thereby enhancing surface quality and lowering forming forces [25, 26]. Duflou et al. [27] highlighted the effectiveness of oils, greases, and waxes as lubricants in ISF, noting mineral oil's prevalent use due to its stable performance. Azevedo et al. [28] observed that the needed lubricant viscosity lessens as sheet hardness increases, while Li et al. [29] found that combining air-dried graphite grease with No. 46 oil enhanced surface quality. Additionally, integrating nanoscale additives into vegetable oil has been shown to increase lubrication by boosting extreme pressure capabilities [30]. This perspective is further supported by Diabb et al. [31]. Şen et al. [32] reported that Minimum Quantity Lubrication (MQL) techniques employing vegetable oils of varied viscosities significantly improved forming quality. High-temperature or pressure conditions often necessitate solid lubricants, such as graphite and molybdenum disulfide [33]. The limited contact area between the tool and the sheet metal tends to cause lubricant extrusion [34], but techniques that improve solid lubricant-sheet adhesion can mitigate this issue, thereby enhancing lubricant efficacy [35]. Zhang et al. [36] enhanced the adhesion of solid graphite and MoS_2 coatings to AZ31 magnesium alloy sheets with $K_2Ti_4O_9$ nanowhiskers and organic binders, showcasing superior lubrication performance. Hussain et al. [37] applied porous titanium oxide coatings on titanium sheets, optimizing storage for

MoS_2 particles and achieving the lowest friction coefficient with a MoS_2-to-grease ratio of 4:1. Astarita et al. [38] suggested that Cold Gas Dynamic Spraying (CGDS) could improve the properties of AA2024 sheets, preventing corrosion and wear. Kilani et al. [39] and Lu et al. [40] highlighted that rolling tools play a crucial role in improving surface quality and formability in ISF, decreasing the need for lubricants. It is evident that extensive and in-depth research on lubricants and lubrication methods is driving the continuous improvement of ISF surface quality. However, the underlying friction mechanisms behind these surface quality enhancements still require further investigation.

The macroscopic interfacial interaction mechanisms are the most direct manifestation of friction behavior in the ISF process. Fan et al. [41] delineated three friction regions in ISF: adhesive friction, boundary lubrication, and fluid lubrication. Reducing adhesive friction is crucial for enhancing surface quality. Silva et al. [42] performed ISF experiments on AA1100 using a hemispherical tool and a two-degree-of-freedom rotating tool, revealing the dominance of the adhesion wear mechanism. In cases of rolling friction, adhesion is localized around the tool contact tip, whereas in sliding friction, adhesion concentrates in the center. Naranjo et al. [43] measured the adhesive layer's thickness on the tool using contour analysis. They theorized that higher forming temperatures exacerbate oxidative wear, creating a friction layer that alters friction behavior. It is evident that the aforementioned studies have characterized interfacial friction behavior through macroscopic surface morphology features. However, the micro-behaviors induced by friction remain underexplored.

Although micro-friction behavior is rarely mentioned in the context of ISF, it has been widely studied in overall forming processes. Shafiee et al. [44] investigated the friction behavior of hot-melt adhesive dry film lubricants in aluminum sheet forming. Through mass spectrometry and X-ray Photoelectron Spectroscopy (XPS) analysis, they speculated on lubricant degradation causing failure, characterized adhesion wear by surface morphology, and identified material transfer from the sheet surface using Energy Dispersive Spectrometer (EDS). Mekicha et al. [45] performed simulations on single roughness, revealing that under lubrication, frictional resistance predominantly stems from matrix deformation. However, in the absence of lubrication, the resistance mainly results from the shearing of adhesive bonds and the tearing of deformed structures. Zhang et al. [46], in their ring compression experiments, found that an increased load leads to lubricant extrusion from the contact surface, diminishing the wedge effect and elevating the proportion of adhesive elements. They also observed that variations in friction result in diverse texture features. Nian et al. [47] reviewed studies on atomic-level transitions, energy dissipation, and bond dynamics at solid interfaces, using first-principles calculations, molecular dynamics, and Atomic Force Microscope (AFM). Their work unveils friction behaviors at the atomic scale. Vorholt et al. [48] crafted an in-situ observation system for stainless steel ironing, discovering that mold surfaces with micro-dimple textures retain lubricating oil, boost load capacity, and generate a fluid dynamic pressure effect. Integrating theoretical and experimental approaches has elucidated interface friction behaviors in traditional sheet metal forming across macro to micro scales. Although the friction characteristics of the dynamic forming process with local cyclic loading in ISF are significantly different from those in overall forming processes, the aforementioned studies provide new insights for revealing the friction behavior in ISF by combining macro- and micro-scale perspectives.

Therefore, to address the current unclear understanding of friction process in ISF, this study experimentally reveals the friction behavior under different friction modes, including interfacial interaction, deformation behavior, and phase evolution, as lubrication conditions vary from good to poor. This research provides a critical scientific foundation for selecting appropriate lubrication conditions and friction modes, aiming to enhance surface quality and formability from a tribological perspective, and seeks to fill the gap in the research on friction behavior in the ISF process.

2 Material and methods

2.1 Material

The study employed AA5052 aluminum alloy sheets, measuring 200 × 200 mm with a 1 mm thickness (*t*), for the incremental forming experiments. The sheets' chemical composition is itemized in Table 1, while their mechanical properties, ascertained via quasi-static tensile testing on an INSTRON-100KN device, are elucidated in Table 2. Tools for sliding and rolling, each with a 7 mm radius (*R*), were fabricated from GCr15 steel, hardened to 64HRC to ensure rigidity during the forming process.

Table 1 Chemical composition of AA5052 (wt%).

Elements	Al	Mg	Cr	Fe	Si	Others
Composition	96.75	2.5	0.25	0.20	0.25	0.05

Table 2 Material properties of AA5052.

ρ (kg/m^3)	E (GPa)	σ_0 (MPa)	UTS (MPa)	Elongation（%）
2680	70.5	100	253.4	20.71

2.2 Experimental Methods

The experimental investigation adopted a single-pass ISF configuration, as schematically presented in Fig. 1(a). A three-axis CNC milling system was programmed to drive a forming tool (radius *R*) along a clockwise truncated-pyramid spiral path with layer-wise downward displacement *Z*, operating at constant feed speed *v* and spindle rotation speed *w*. A metallic sheet with nominal thickness *t* was rigidly clamped between a matched-die set comprising an upper blank holder and lower backing plate. Through progressive accumulation of localized plastic deformation, the system successfully fabricated a truncated pyramid geometry featuring a wall inclination angle $\alpha = 50°$, with specified dimensions of 100 mm opening diameter and 50 mm forming depth, as demonstrated in Fig. 1(d). A three-dimensional force sensor was utilized to record real-time forming forces (F_x, F_y, F_z) along the x-, y-, and z-axes. Simultaneous thermal monitoring was performed throughout the forming process using an infrared thermal imager.

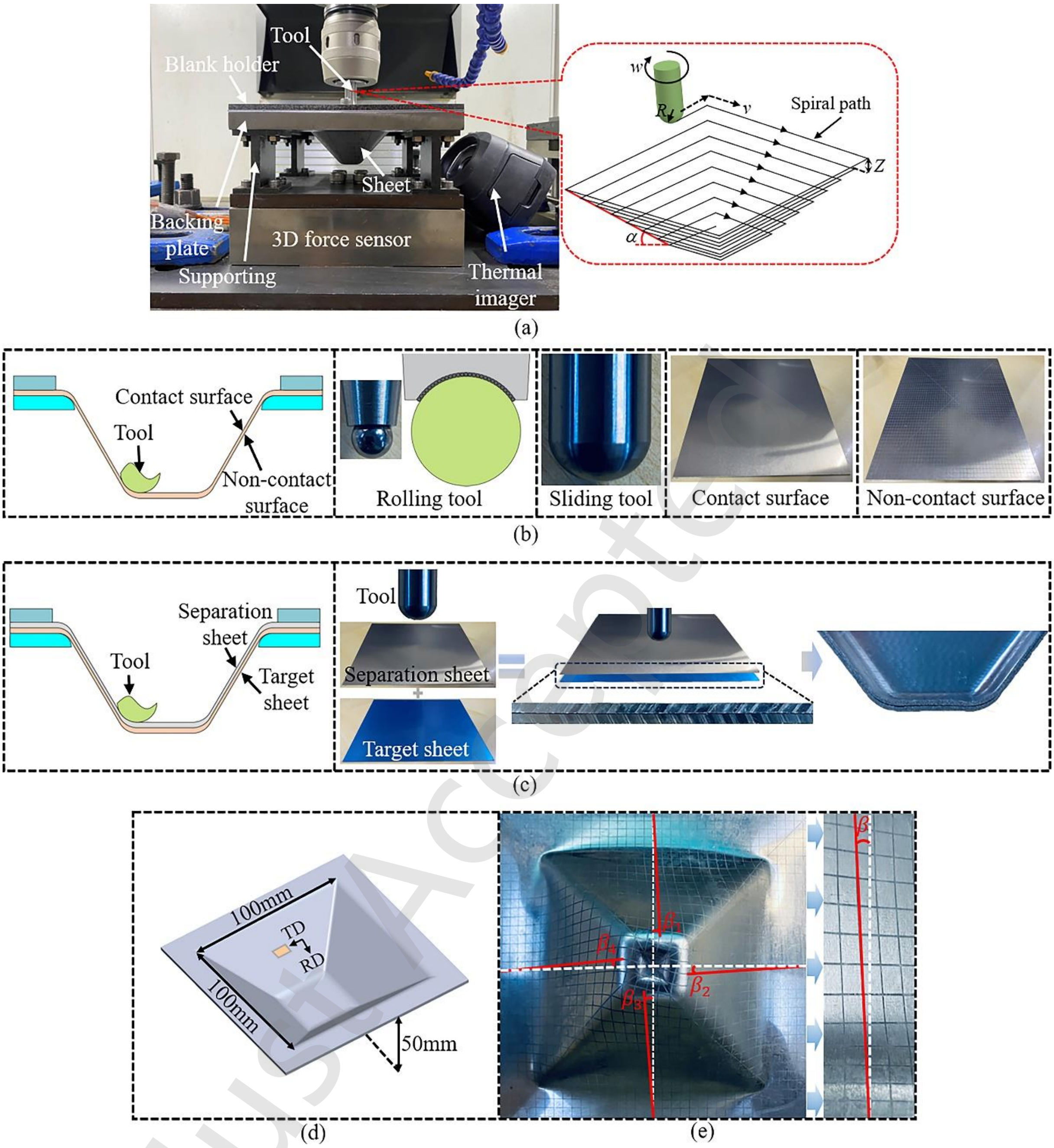

Fig. 1 (a) Friction test system of incremental sheet forming; (b) schematic of incremental sheet forming with rolling and sliding friction; (c) schematic of incremental sheet forming with free deformation; (d) schematic diagram showing the position and orientation of the test specimen for surface morphology, microstructure, and phase information detection on the part; (e) schematic diagram of part twist angle measurement.

The principle of ISF with friction, as depicted in Fig. 1(b), involves direct compressive contact between the tool and the sheet metal, where the type of tool used dictates the friction mode during the forming process. Utilizing a freely rotating spherical tool induces rolling friction between the tool and sheet metal, characterizing the incremental sheet forming with rolling friction (ISF-RF) process. Conversely, employing a semispherical tool results in sliding friction, defining the incremental sheet forming with sliding friction (ISF-SF) process. The initial contact surface of the sheet metal was smooth and unscratched, while the non-contact surface underwent chemical etching with a 4 × 4mm grid for deformation analysis.

Critical experimental parameters are delineated in Table 3, highlighting the main components, properties, and suitable working conditions of hydraulic oil [49], MoS_2 grease, and graphite powder, as shown in Table 4. These lubricants are archetypical representatives of liquid, grease, and solid lubricants, respectively, extensively utilized in sheet metal forming. Exploring dry friction conditions without lubrication enriches the understanding of friction behavior in ISF.

Table 3 Experimental process parameters.

	ISF-SF	ISF-RF	ISF-FD
Lubricant	Hydraulic oil MoS_2 grease Graphite powder Dry	Hydraulic oil MoS_2 grease Graphite powder Dry	Hydraulic oil
Rotation speed w (rpm)	500	Free rotation	Free rotation
Feed speed v (mm/min)	1000	1000	1000
Layer-downward displacement Z (mm)	0.5	0.5	0.5
Wall inclination angle α (°)	50	50	50
Sheet thickness t (mm)	1	1	1
Tool radius R (mm)	7	7	7
Process path	Spiral path	Spiral path	Spiral path

Table 4 Lubricant properties and applications.

	Main components	Properties	Suitable working conditions
Hydraulic oil	Mineral base oil Additives	Kinematic viscosity at 40°C: 46.6 mm²/s Viscosity index: 101 Flash point: 238°C Pour point: -15°C Suitable temperature range: -20°C to 80°C	High-speed operating conditions
MoS_2 grease	Inorganic thickener thickened synthetic oil grease MoS_2 solid lubricant Other Additives	Dropping point: 480°C Consistency grade: NLGI 2 Suitable temperature range: -30°C to 380°C	High-temperature and high-pressure operating conditions
Graphite powder	Graphite powder particles	Diameter: 100 nm Purity: 99.9% Natural flake graphite Melting point: ~3650°C Boiling point: ~4200°C Thermal stability: above 3000°C	High-temperature, high-pressure, and vacuum operating conditions

Rolling and sliding friction represent two quintessential friction modes in incremental sheet forming (ISF). Exploring their friction behaviors provides a basis for in-depth study of ISF processes from a tribological perspective under typical lubrication conditions. In the nearly friction-free incremental sheet forming with free deformation (ISF-FD) process, the target sheet is subjected almost exclusively to compressive deformation, with minimal frictional influence. Therefore, its deformation characteristics can serve as a reference for comparison with ISF-RF and ISF-SF processes, avoiding the erroneous attribution of compressive deformation effects to friction effects. The principle of ISF-FD forming is illustrated in Fig. 1(c). In this process, a separating sheet with the same material properties as the target sheet is placed between the tool and the target sheet, and a highly elastic PE protective film coated with hydraulic oil lubricant is applied on the surface of the target sheet. The deformation compatibility between the non-contact side of the separating sheet and the PE protective film in close contact with it results in minimal relative motion between them. Furthermore, the lubricant further diminishes potential friction effects. Through this protective mechanism, the target sheet achieves nearly friction-free free plastic deformation during the ISF process.

2.3 Characterization Methods

The friction force f in ISF is determined by integrating the shear stress over the deformed contact area S, where the shear stress is governed by the friction coefficient μ and the normal stress σ_t at the tool-sheet interface, as expressed in Eq. (1). Notably, the friction force primarily acts along the horizontal plane and corresponds to the vector difference between the horizontal forming force F_{xy} and the material deformation resistance F_d, as formulated in Eq. (2). By establishing equilibrium between Eqs. (1) and (2), the friction coefficient μ during ISF can be quantitatively determined, as derived in Eq. (3) [50, 51].

$$f = \mu \sigma_t S \tag{1}$$

$$f = \bar{F}_{xy} - \bar{F}_d \tag{2}$$

$$\mu = \frac{\bar{F}_{xy} - \bar{F}_h}{\sigma_t S} \tag{3}$$

Where F_{xy} can be determined through the x-axis force component F_x and the y-axis force component F_y, as shown in Eq. (4).

$$F_{xy} = \sqrt{F_x^2 + F_y^2} \tag{4}$$

A thermal camera was used to obtain one temperature data point at the middle position of each forming layer, considering the highest temperature in the contact area between the tool and the sheet as the temperature of that forming layer. This process was repeated to collect forming temperature data for each of the 100 forming layers of each part. The average temperature during the steady-state stage was considered the forming temperature under the corresponding forming conditions. Due to the complexity and lack of a well-defined reflective surface in the direct contact zone between the tool and sheet, significant measurement errors occurred. Additionally, because the sheet is thin and has good thermal conductivity, measurements were taken on the non-contact surface aligned with the sheet's contact area, which provided improved conditions for reflective measurements, as depicted in Fig. 1a (with a deviation of no more than 5℃ from the contact surface forming temperature).

The material located at the central region of the part's sidewall was prepared into specimens for surface morphology and microstructure characterization, as illustrated in Fig. 1(d). The specimen's thickness direction is defined as Normal Direction (ND), the stretching direction as Rolling Direction (RD), and the feed direction as Transverse Direction (TD). The specimen was ultrasonically cleaned in acetone for half an hour, followed by anhydrous ethanol for an hour before air drying. Surface morphology was observed using a Scanning Electron Microscope (SEM). The main chemical composition of the specimen surfaces was determined using an Energy Dispersive Spectrometer (EDS). X-ray Diffraction (XRD) was used to analyze the surface phase and crystal orientation. X-ray Photoelectron Spectroscopy (XPS) characterized the elemental composition and chemical states of the surface layer. Electron Backscatter Diffraction (EBSD) characterized the microcrystalline structure of the surface layer.

The tangential friction between the tool and the sheet induces shear strain on the sheet's surface, causing a shear deformation and a macroscopic geometric twist. This twist is illustrated by the deformation of a square grid on the part's surface, as shown in Fig. 1(e). The grid lines, initially straight, undergo angular displacement post-twist. By measuring the twist angles (β_1, β_2, β_3, and β_4) on the part's four sidewalls and calculating their average with Eq. (5), this average is taken as the mean twist angle (β).

$$\beta = \frac{\beta_1 + \beta_2 + \beta_3 + \beta_4}{4} \tag{5}$$

Surface morphological characteristics, phase composition, microstructural organization, and shear deformation influence the performance of ISF, while the maximum forming angle (α_{max}) serves as a key indicator for evaluating the formability of this process. To investigate this, incremental forming experiments on sheet metal were conducted under varying friction modes and lubrication conditions. During the experiments, the forming wall inclination angle was incrementally increased from 0° until fracture occurred. The forming wall inclination angle at the fracture location of the formed part was defined as the maximum forming angle (α_{max}) under the corresponding forming conditions.

3 Results

3.1 Friction coefficient and forming temperature

As shown in Fig. 2(a), the friction coefficient increases gradually under various forming conditions and then remains relatively stable once it enters the steady-state stage. The average friction coefficient during the steady-state stage is considered the friction coefficient for the corresponding forming condition. Specifically, oil lubrication yields the lowest friction coefficients for both ISF-SF (0.1901) and ISF-RF (0.0957). Transitioning to grease lubrication, the friction coefficient rises by 14.361% in ISF-SF and 39.707% in ISF-RF. Powder lubrication further escalates the coefficients by 70.437% for ISF-SF and 109.613% for ISF-RF. Under dry conditions, the increases peak at 134.666% for ISF-SF and 117.346% for ISF-RF. These results reveal a consistent increase from oil to dry lubrication, with ISF-SF consistently exhibiting higher coefficients than ISF-RF under identical lubrication scenarios.

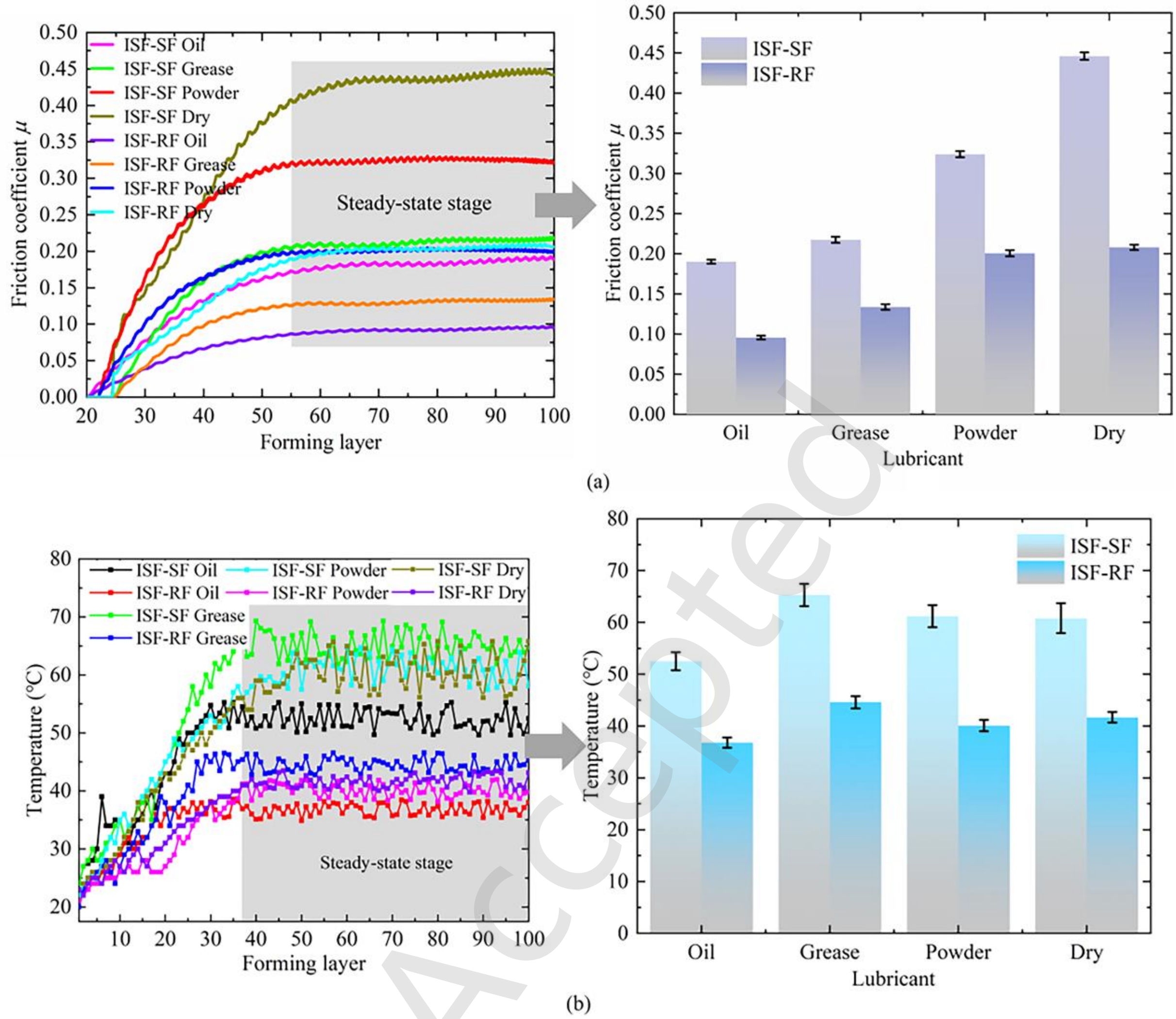

Fig. 2 (a) Friction coefficient μ. ; (b) forming temperature.

As shown in Fig. 2(b), the forming temperature increases gradually under various forming conditions and then remains relatively stable once it enters the steady-state stage. The average forming temperature during the steady-state stage is considered the forming temperature for the corresponding forming condition. During ISF-SF and ISF-RF, the temperatures observed under oil lubrication are 52.5°C and 36.8°C, respectively, indicating that the oil's performance is unlikely to be significantly affected within this temperature range. Under grease lubrication, temperatures rise to 65.3°C for ISF-SF and 44.6°C for ISF-RF. For powder lubrication, the respective temperatures are 61.2°C and 40.1°C, while dry friction conditions yield temperatures of 60.8°C and 41.7°C during ISF-SF and ISF-RF. The data suggest that oil lubrication not only serves as an effective lubricant but also enhances heat dissipation, thereby lowering temperatures in the forming area. Conversely, the high density and limited flowability of grease impede heat dissipation, resulting in elevated forming temperatures. Powder lubrication suffers from poor adherence to both tool and sheet, leading to increased friction and heat generation. Dry friction, lacking lubrication, further exacerbates frictional heat. Nonetheless, temperatures under powder lubrication and dry friction remain lower than those observed with grease lubrication, thanks to more favorable heat dissipation conditions. Furthermore, it is noted that temperatures during ISF-RF are consistently lower than those during ISF-SF. This phenomenon is attributed to reduced sliding between tool and sheet in ISF-RF, which minimizes frictional heat production. In contrast, ISF-SF involves the tool sliding over the sheet at a feed speed of 1000 mm/min and a rotation speed of 500 rpm, generating higher frictional heat and consequently, increased forming temperatures.

3.2 Surface morphology and phase

The surface morphology of specimens formed through ISF-FD is depicted in Fig. 3(a). Remarkably, the surface is devoid of friction marks, though traces of considerable plastic deformation are present. This deformation triggers widespread dislocation motion within the material, leading to dislocation emergence at surface grain boundaries, which is macroscopically observed as surface roughening. The primary chemical composition of the surface, detailed in Figs. 3(b), (c), reveals the presence of aluminum (Al) and magnesium (Mg), which are characteristic components of the AA5052 alloy. Additionally, oxygen (O) and carbon (C) are detected. The increase in O content signifies surface oxidation, resulting in the formation of oxide layers. The presence of C suggests contamination from organic sources.

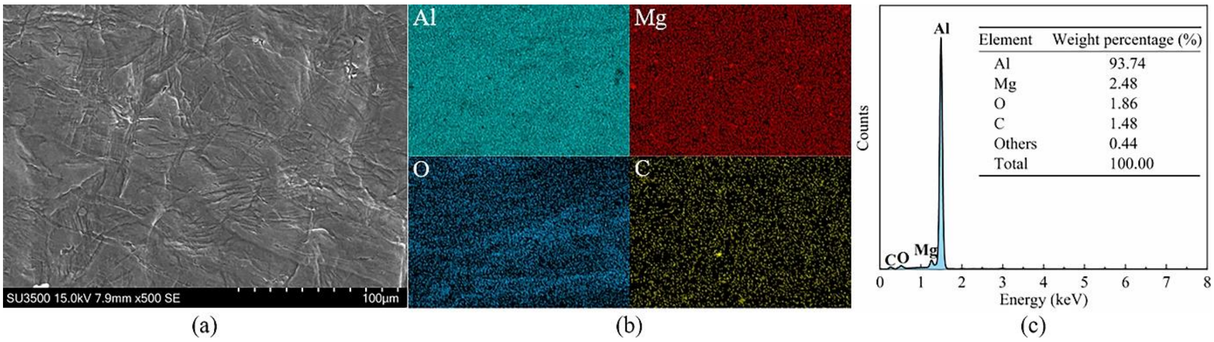

Fig. 3 (a) Surface morphology of specimen formed through ISF-FD; (b) surface elements; (c) surface elemental composition.

The surface morphology of specimens formed by ISF-RF is depicted in Fig. 4. In the case of oil lubrication, the surface features closely resemble those of ISF-FD, displaying distinct traces of plastic deformation. Additionally, traces of surface material folding are evident. The use of grease lubrication results in similar observations, with the addition of scattered, flake-like debris on the surface. When employing powder lubrication or forming under dry friction conditions, the severity of material folding, termed extrusion folding, intensifies. This phenomenon is marked by a remarkable increase in the depth and breadth of the folds, coupled with a higher prevalence of flake-like debris. Additionally, the surface exhibits tough tear pits, indicating more aggressive wear and deformation under these conditions.

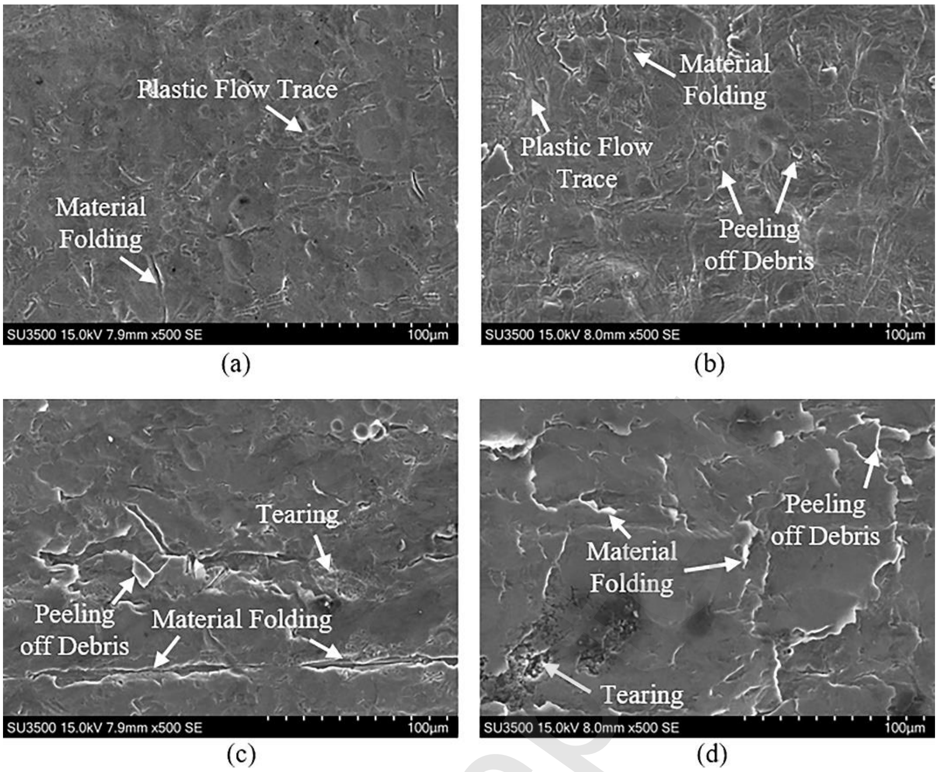

Fig. 4 Surface morphology of specimens formed by ISF-RF: (a) oil; (b) grease; (c) powder; (d) dry friction.

The surface morphology of the specimen formed via ISF-SF is illustrated in Fig. 5. With oil and grease used as lubricants, the tool's movement across the sheet at a feed speed of 1000 mm/min and a rotation speed of 500 rpm results in distinctive ripple-like deformation patterns, scratches, and material folding visible on the surface. Additionally, the surface features include tearing pits and flake-like debris that have not been completely peeled off. Microcracks are also observable on the surface, as depicted in Figs. 5(a), (b). With the application of powder lubrication, the surface is characterized by an abundance of blocky and granular debris and tearing and layered fracture defects within the surface material, as demonstrated in Fig. 5(c). Under dry friction conditions, the interaction between the tool and sheet becomes more severe, exacerbating the depth of fracture defects, enlarging the size of fractured debris, and leading to the embedding of some debris within the fracture pits, thus resulting in a markedly poor surface quality, as shown in Fig. 5(d).

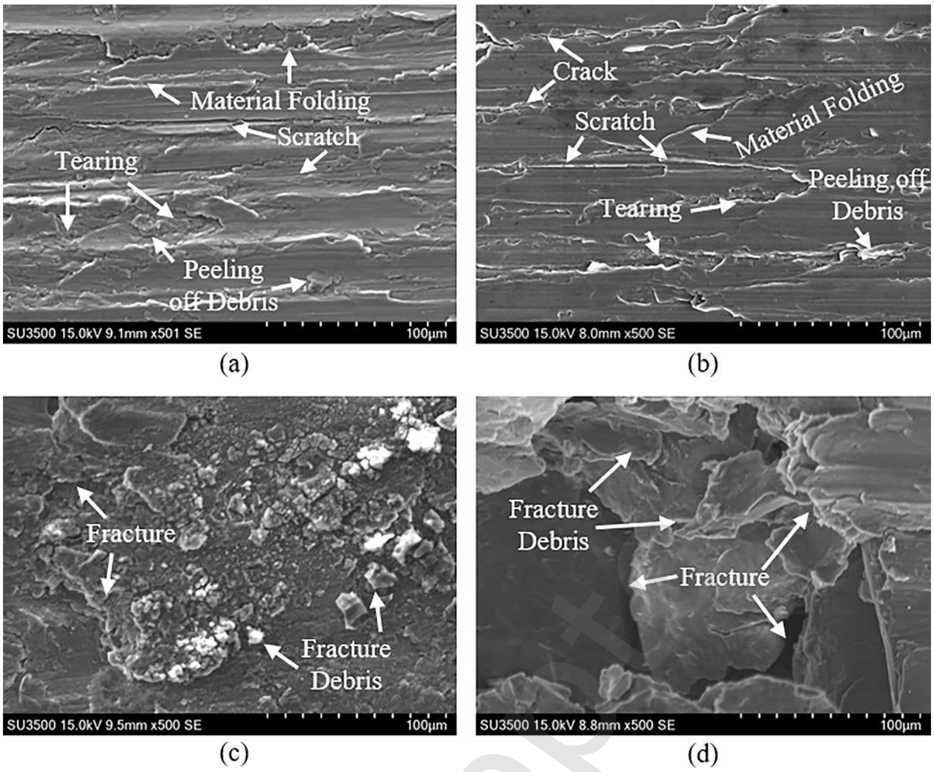

Fig. 5 Surface morphology of specimens formed by ISF-SF: (a) oil; (b) grease; (c) powder; (d) dry friction.

Comparative analysis of surface O content from specimens formed by ISF-FD (Fig. 3(c)) and those formed by ISF with friction (Fig. 6) reveals a general increase in surface O content in the latter. Specifically, for specimens formed by ISF-RF, the surface O contents under oil, grease, powder, and dry friction conditions are recorded at 1.87%, 1.98%, 5.88%, and 6.82%, respectively. By contrast, for ISF-SF under the same lubrication conditions, the surface O contents are markedly higher: 6.67%, 8.17%, 27.92%, and 30.22%, respectively. This pattern suggests a correlation between the variation in friction coefficients and the surface O content across different friction modes. Specifically, the surface O content is minimal with oil lubrication, slightly higher with grease, and substantially increases under powder lubrication and dry friction conditions. Furthermore, the surface O content for specimens formed by ISF-RF is considerably lower than those formed by ISF-SF under comparable lubrication conditions, indicating that the forming technique affects the extent of surface oxidation.

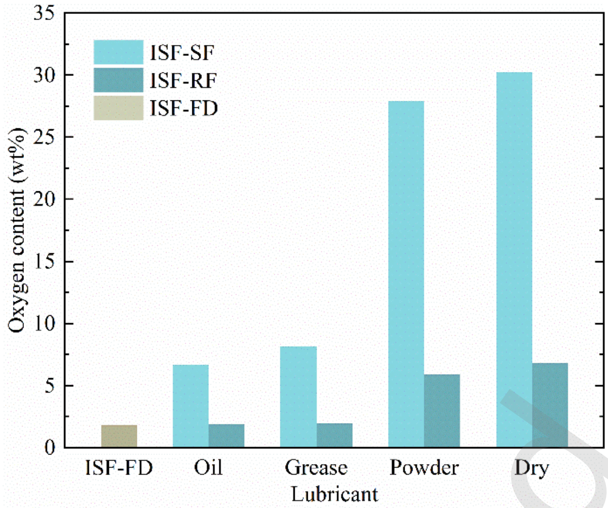

Fig. 6 Surface oxygen content in incremental sheet forming under different lubrication conditions and friction modes.

The XPS results, as depicted in Fig. 7, detail the chemical composition of surfaces from specimens created by ISF-FD, ISF-RF, and ISF-SF under oil lubrication and dry friction conditions. Similar to EDS results, XPS detects Al and Mg, as well as O and C, from the AA5052 alloy, as shown in Fig. 7(a). While slight discrepancies in element percentages between XPS and EDS may arise due to differences in detection principles, settings, and methodologies, a consistent trend in O content is observed: it is lowest for ISF-FD, lower under oil lubrication compared with dry friction, and higher during ISF-SF than ISF-RF under identical lubrication conditions. This trend suggests that the continuous exposure of new surfaces during forming reacts with atmospheric oxygen, leading to oxidation and the formation of metal oxides. Further exploration of surface compound composition through element-specific spectra is depicted in Figs. 7(b)-(e). The C spectrum (Fig. 7(b)) confirms the presence of C-C and C-O bonds, indicating organic contamination. The Al spectrum (Fig. 7(c)) reveals that in addition to minor elemental Al, it primarily consists of aluminum oxide (Al_2O_3). The Mg spectrum (Fig. 7(d)) indicates a composition largely of magnesium oxide (MgO), with some elemental Mg. The detailed spectrum of O (Fig. 7(e)) suggests its involvement in forming Al_2O_3 and MgO, in addition to potential organic contamination. That is, the main products of increased surface oxygen are metal oxides. This indicates that during ISF, under the same friction conditions, the metal oxide content is higher in dry friction compared with oil lubrication. Additionally, under the same lubrication conditions, the metal oxide content is higher in ISF-SF than in ISF-RF. This again demonstrates through data the effect of friction modes and lubrication conditions on the surface oxide content during ISF.

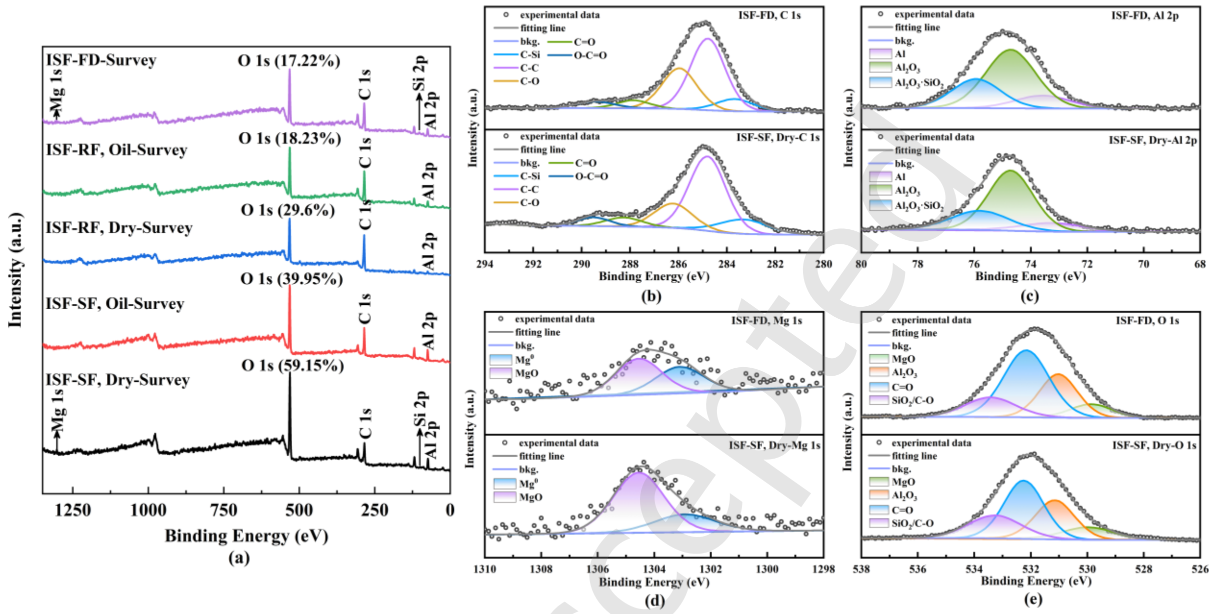

Fig. 7 Phase analysis of formed specimens by incremental sheet forming under different lubrication conditions and friction modes: (a) survey spectrum; (b) C element spectrum; (c) Al element spectru; (d) Mg element spectrum; (e) O element spectrum.

3.3 Microstructure characterization

The surface characteristics of parts formed under different conditions and the as-received material were examined using XRD, as shown in Fig. 8. The as-received material exhibits remarkable peak intensities at the (111), (200), and (220) crystal planes, indicating no remarkable orientation in the as-received material. Within the context of ISF-FD, the surface exhibits peak intensity at the (220) crystal plane. This trend persists in ISF-RF, where the (220) crystal plane similarly showcases the most pronounced peak, suggesting that rolling friction exerts minimal influence on the orientation of surface grains. Here, the predominant factor is the rotation of the crystal lattice, which is a consequence of extrusion plastic deformation. In the scenario of ISF-SF employing oil lubrication, while the (220) crystal plane continues to display the highest intensity, the intensity of the (200) crystal plane remarkably increases. Under dry friction conditions, however, the surface grains predominantly exhibit the strongest peak at the (200) crystal plane. This observation underscores that the frictional conditions inherent to ISF-SF considerably influence the orientation of surface grains, leading to a shift from the deformation-induced (220) orientation to the (200) crystal plane.

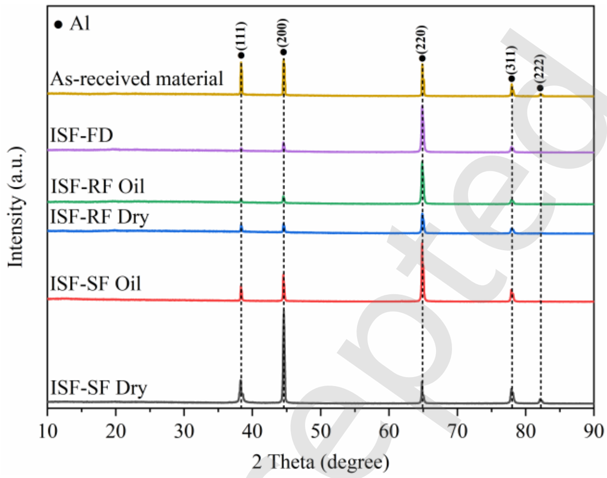

Fig. 8 Surface crystal structure of formed specimens by incremental sheet forming under different friction modes and lubrication conditions detected by X-ray diffraction.

Fig. 9(a) displays the inverse pole figure (IPF) obtained from EBSD analysis for the surface of the specimen formed by ISF-FD. The microstructural analysis of the surface, as illustrated in Fig. 9(b), demonstrates pronounced {110} texture characteristics, considerably characterized by Brass {110}<112> and {110}<110> orientations. The Orientation Distribution Function (ODF) map, shown in Fig. 9c, corroborates these findings, further confirming the distinct texture characteristics of the surface.

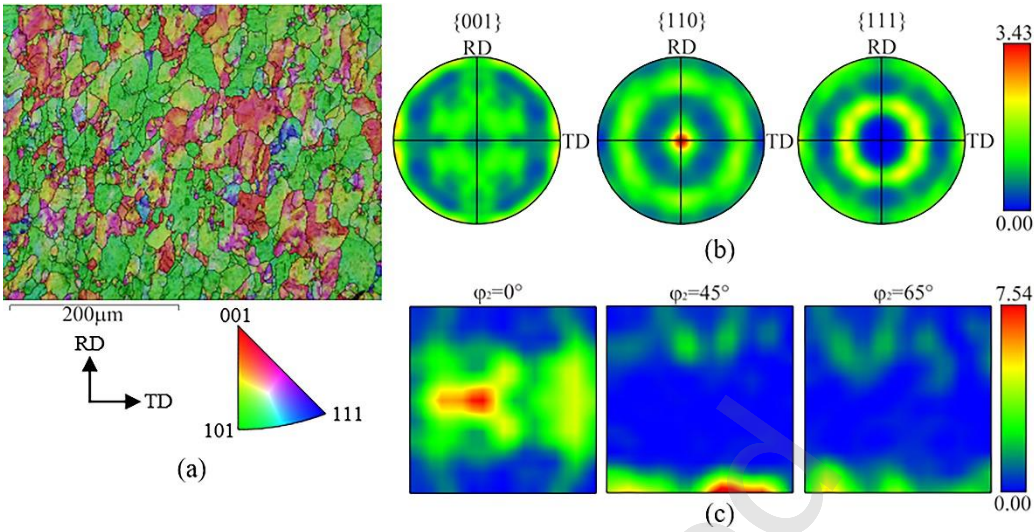

Fig. 9 EBSD results of ISF-FD: (a) IPF map; (b) PF map; (c) ODF map.

In the context of ISF-RF, EBSD results for the specimens formed under oil lubrication and dry friction conditions are detailed in Fig. 10. As shown in Fig. 10(a) and (d), the IPF indicates that the number of intragranular subgrains is greater under dry friction conditions than under oil lubrication conditions. Furthermore, compared with Fig. 9(a), more intragranular subgrains are observed during rolling friction than during ISF-FD. Pole figures corresponding to oil lubrication and dry friction conditions are illustrated in Figs. 10(b) and (e), respectively. The ODF maps, shown in Figs. 10(c) and (f), are both predominantly characterized by the {110} texture. Under oil lubrication, the Brass {110}<112> texture is prominent, followed by the Goss {110}<001> and Copper {112}<111> textures. Under dry friction conditions, the Brass {110}<112> texture remains dominant, with notable contributions from the {110}<110> and Copper {112}<111> textures. These observations indicate that rolling friction does not alter the orientation of most grains in the surface layer during incremental forming, which is still dominated by the {110} texture, and only induces a small portion of the grains in the surface layers to rotate toward the Copper {112}<111> texture.

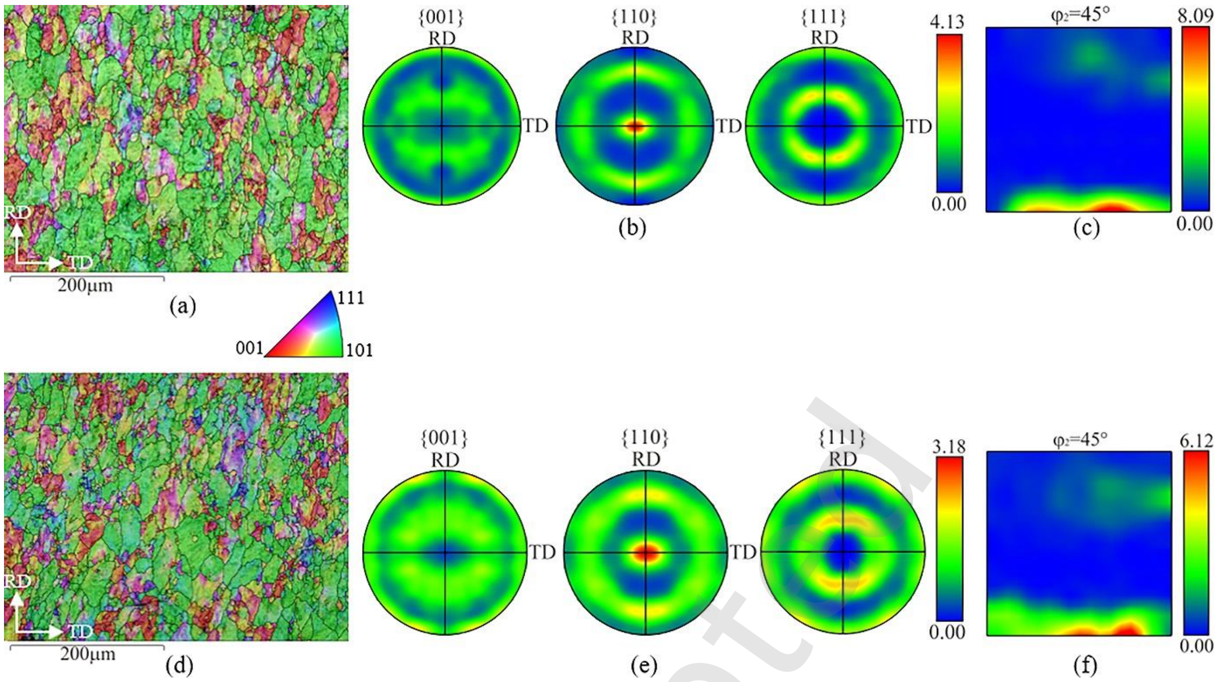

Fig. 10 EBSD results of ISF-RF: (a)-(c) microstructure of the surface layer in specimen formed under oil lubrication; (d)-(f) microstructure of the surface layer in specimen formed under dry friction.

In the scenario of ISF-SF subjected to oil lubrication and dry friction conditions, the EBSD results are showcased in Fig. 11. As shown in Fig. 11(a) and (d), the IPF reveals that under dry friction conditions, the number of intragranular subgrains remarkably increases in comparison with those under oil lubrication conditions. Under oil lubrication, the surface layer maintains a significant {110} texture, predominantly characterized by Brass {110}<112> and {110}<110> textures, with the presence of a notable {001}<100> cubic texture, as indicated in Figs. 11(b) and (c). By contrast, under dry friction conditions, the {001}<100> cubic texture becomes the most pronounced in the surface layer, overtaking the {110} texture, as demonstrated in Figs. 11(e), (f), where the Copper {112}<111> texture also makes an appearance. These observations highlight that sliding friction causes a shift in the orientation of surface layer grains towards the cubic texture {001}<100>, with increased sliding friction further facilitating the emergence of the Copper {112}<111> texture.

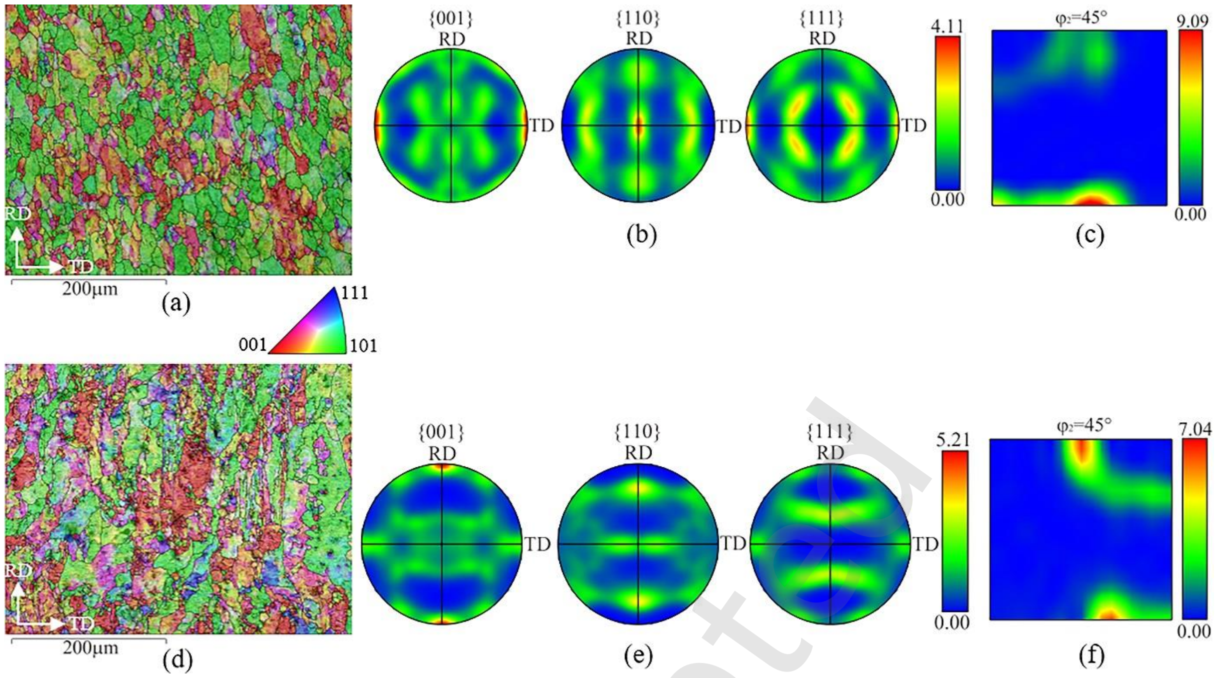

Fig. 11 EBSD results of ISF-SF: (a)-(c) microstructure of the surface layer in specimen formed under oil lubrication; (d)-(f) microstructure of the surface layer in specimen formed under dry friction.

The average grain sizes under different friction modes and lubrication conditions are shown in Fig. 12. The grain size during ISF-FD is the largest, at 15.9 μm. When friction is present, the grain size decreases to varying degrees. With oil lubrication, the grain size under rolling friction is 11.25 μm, while under sliding friction it is 10.44 μm. Under dry friction conditions, the grain size is 9.45 μm for rolling friction and 7.4 μm for sliding friction. Under the same lubrication conditions, the grain size is smaller for sliding friction compared with rolling friction. Additionally, for the same mode of friction, the grain size under dry friction conditions is considerably smaller than that under oil lubrication.

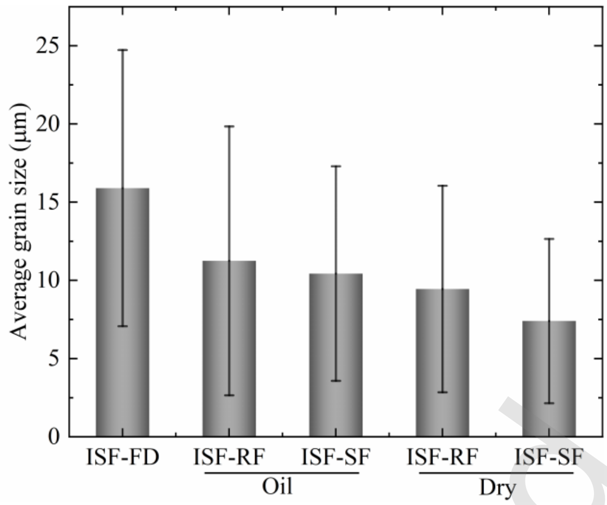

Fig. 12 Average grain size in incremental sheet forming under different friction modes and lubrication conditions.

The geometric dislocation density serves as a baseline measure for the surface dislocation density and is utilized to evaluate the microstructural dislocation density of the surface layer in incremental forming specimens under varying friction conditions. To obtain this parameter, the crystal orientation differences between adjacent grains were calculated using AztecCrystal software. These orientation differences were used to estimate the geometrically necessary dislocation (GND) density of each grain. The average GND density for all grains in the observation area is shown in Fig. 13(a). Without friction, the GND density reaches its lowest value of 2.09. However, with the introduction of friction in ISF, a discernible increase in surface dislocation density is observed. Specifically, in ISF-RF, the GND densities under oil lubrication and dry friction are recorded at 2.15 and 2.3, respectively. Meanwhile, in ISF-SF, these densities increase to 2.25 and 2.64 under oil lubrication and dry friction, respectively. This trend clearly indicates that the dislocation density is lower under oil lubrication than under dry friction within the same mode of friction. Moreover, the dislocation density associated with sliding friction surpasses that observed with rolling friction, given identical lubrication conditions.

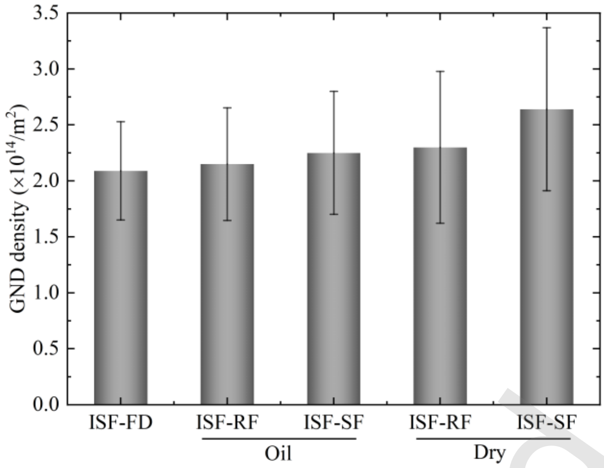

Fig. 13 Geometric dislocation density on the surface of formed specimens by incremental sheet forming under different friction modes and lubrication conditions.

3.4 Forming Performance

The predominant factor causing geometric twist in specimens is the shear deformation. The twist angle (β) of specimens under various lubrication conditions and friction modes is illustrated in Fig. 14(a). In ISF-FD, a minimal twist angle resulting from free plastic deformation is noted, with a value of 0.309°. However, under oil lubrication, grease lubrication, powder lubrication, and dry friction conditions, the twist angles for ISF-RF are observed to be 0.405°, 0.64°, 0.962°, and 0.98°, respectively. For ISF-SF, the corresponding twist angles are remarkably higher, recorded at 1.752°, 1.88°, 2.235°, and 2.435°. This result demonstrates that the friction effects lead to an increase in the twist angle of the specimen, and as the friction effects intensify, the macroscopic geometric twist angle also escalates proportionally. Additionally, under the same lubrication conditions, the twist angle in ISF-RF is markedly lower than that in ISF-SF. This difference is attributable to the weak effects of rolling friction because the rolling tool undergoes minimal relative sliding with the material in the deformation zone. In ISF-SF, the direction of friction shear strain, which impacts the macroscopic twist angle, is determined by the combined sliding movements due to the tool's rotational and feed motions. Notably, in this study, the rotational and feed directions of the tool are counterclockwise, with the analysis not extending to combinations of differing motion directions.

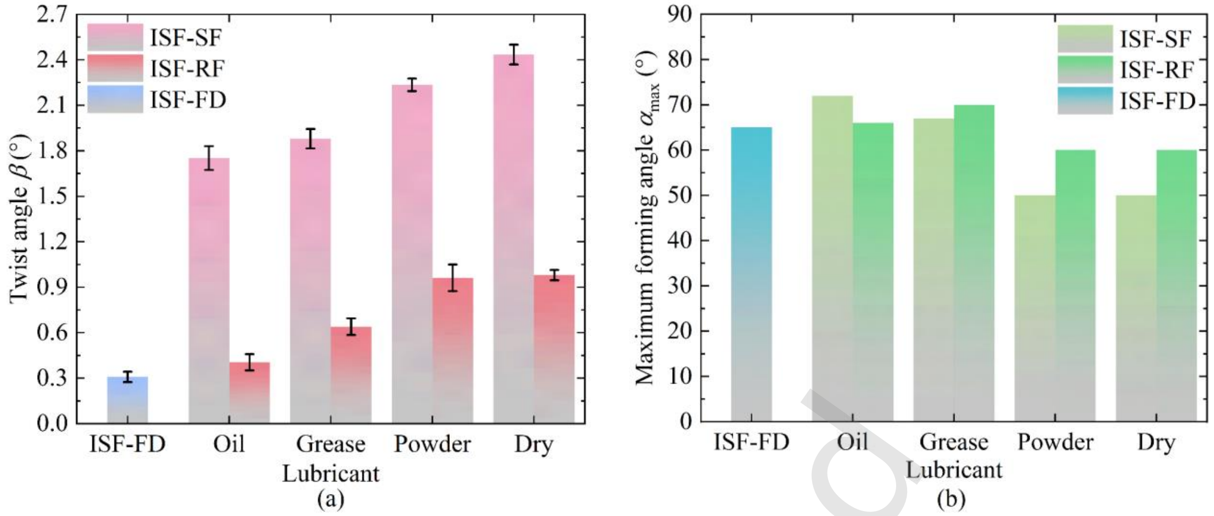

Fig. 14 Forming performance of incremental sheet forming under different friction modes and lubrication conditions: (a) twist angle β; (b) maximum forming angle α_{max}.

The microstructural characteristics, shear strain, and surface morphology considerably influence the performance of incremental forming processes, with the maximum forming angle (α_{max}) serving as a pivotal metric for evaluating performance. Fig. 14(b) illustrates the maximum forming angles achieved under various lubrication conditions. Specifically, for ISF-RF, the maximum forming angles under oil lubrication, grease lubrication, powder lubrication, and dry friction conditions are recorded at 66°, 70°, 60°, and 60°, respectively. For ISF-SF, these angles are 72°, 67°, 50°, and 50°, respectively. In the absence of any friction, a baseline maximum forming angle of 65° is observed. These data reveal a nuanced relationship between the friction coefficient and the maximum forming angle in ISF-RF, where the angle initially increases with an increase in friction, followed by a decrease as the friction coefficient continues to rise. By contrast, within the ISF-SF process, the maximum forming angle consistently decreases as the friction coefficient increases. When compared with ISF-FD, it becomes apparent that a moderate increase in rolling friction can improve the maximum forming angle, thereby enhancing the forming performance. However, an excessively high rolling friction diminishes the maximum forming angle, indicating a decline in forming capabilities. Similarly, a lower sliding friction can augment the forming performance by increasing the maximum forming angle, whereas a higher sliding friction detrimentally affects the performance, reducing the maximum forming angle. In summary, across both friction modes, lower friction coefficients demonstrate a mild friction effect that beneficially influences forming performance. Conversely, higher friction coefficients result in a marked decrease in forming performance, primarily due to pronounced friction effects.

4 Discussion

4.1 Additional deformation behavior under different friction modes

During ISF-RF, the rolling tool induces local plastic deformation by extruding the sheet metal, creating a rolling frictional traction force as the surface material flows plastically and drives the rolling tool to rotate in tandem with the plastic flow of the surface material. Hence, the friction mode between the rolling tool and the sheet metal is referred to as rolling friction. As illustrated in Fig. 4, the surface morphology of parts formed by ISF-RF does not exhibit distinct orientation deformation features, resembling the deformation surface morphology shown in Fig. 3(a), which is affected almost exclusively by extrusion deformation with minimal friction effect in ISF-FD. During ISF-RF, the frictional force induces non-directional additional shear deformation. In other words, the rolling friction direction changes with the rolling tool's rotation, leading to non-directional friction flow lines, as depicted in Fig. 15.

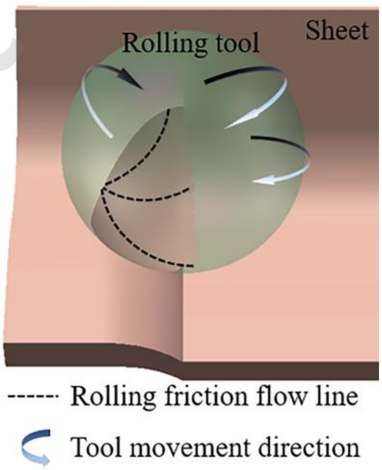

Fig. 15 Schematic of rolling friction flow line during incremental sheet forming with rolling friction.

As shown in Fig. 8, the XRD results for ISF-FD reveal that extrusion deformation, with minimal frictional influence, induces a pronounced crystallographic texture parallel to the (220) crystal plane in the originally non-directional crystal structure. However, the XRD results for ISF-RF are consistent with those for ISF-FD, indicating that the rolling friction introduces non-directional shear deformation, thus not altering the (220) crystal plane orientation parallel to the {110} plane induced by extrusion deformation. Moreover, a comparative analysis of the EBSD results shown in Figs. 9 and 10 reveals that ISF-RF does not change the crystallographic orientation of the surface material, maintaining the {110} texture (primarily Brass {110}<112> and {110}<110>), with a weaker Copper {112}<111> texture, similar to that produced by extrusion deformation in ISF-FD. This result further corroborates that the non-directional shear deformation introduced by rolling friction does not affect the grain orientation induced by the extrusion deformation inherent in the ISF process.

Given that the non-directional rolling friction effect in ISF-RF generates non-directional shear deformation with a smaller component in the feed direction, as shown in Fig. 14(a), the increase in the twist angle for ISF-RF is not remarkable compared to the twist angle dominated by extrusion deformation in ISF-FD (twist angle of 0.309°). This is particularly true under conditions of weak friction effects, such as oil lubrication, where the twist angle is only 0.405°, which is less than that observed in ISF-SF.

During ISF-SF, the sliding tool employs a combined motion of active feed and rotational movements to slide and extrude the sheet metal layer by layer. Thus, in addition to the extruded plastic deformation, the surface material of the sheet is subjected to additional shear deformation induced by sliding friction in the feed direction. As shown in Fig. 5, the surface of the sheet metal formed by sliding friction (with oil and grease lubrication) exhibits distinct deformation features along the feed direction, which is considerably different from the non-directional deformation characteristics depicted in Figs. 3(a) and 4. During ISF-SF, the frictional force induces directional additional shear deformation, with the sliding friction direction aligned with the feed direction. Consequently, the friction flow lines are as shown in Fig. 16. This directional sliding friction effect leaves wavy deformation patterns between adjacent forming layers, as illustrated in Figs. 5(a) and (b).

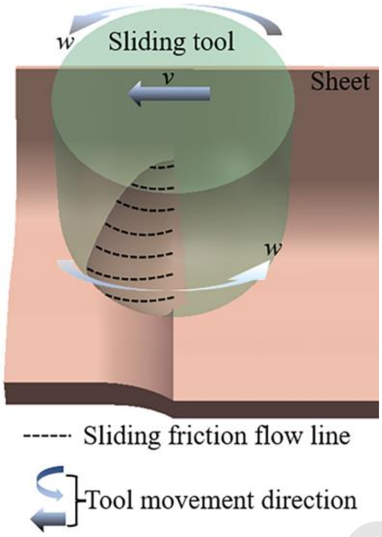

Fig. 16 Schematic of sliding friction flow line during incremental sheet forming with silding friction.

As shown in Fig. 8, the XRD results for ISF-SF reveal crystal structure characteristics with increasingly strong peaks parallel to the (200) crystal plane of the {001} family. This outcome is notably different from the crystal structure oriented parallel to the (220) plane produced by extrusion deformation in ISF-FD and ISF-RF. This finding indicates that sliding friction introduces directional shear deformation, causing the crystal structure, originally oriented parallel to the (220) plane due to extrusion deformation, to shift toward an orientation parallel to the (200) plane. Additionally, a comparative analysis of the EBSD results for ISF-SF in Fig. 11 with those for ISF-FD and ISF-RF in Figs. 9 and 10 shows that ISF-SF considerably alters the surface crystal orientation. The texture dominated by the {110} plane due to extrusion deformation transitions to a cubic texture dominated by {001}<100>. This transition further confirms that the directional shear deformation introduced by sliding friction shifts the grain orientation from the {110} texture induced by extrusion deformation in the ISF process to a {001} texture.

Given that the directional shear deformation effect generated by the directional sliding friction in ISF-SF aligns with the feed direction, as shown in Fig. 14(a), the increase in the twist angle for ISF-SF is considerably more pronounced in comparison with the twist angles in ISF-FD and ISF-RF, which are dominated by extrusion deformation.

4.2 Interfacial effects under different lubrication conditions

Similar to the surface morphology characteristics of the ISF-FD formed parts shown in Fig. 3, the surface of ISF-RF formed parts under oil lubrication, as shown in Fig. 4(a), also exhibits noticeable roughening due to plastic deformation caused by extrusion forces. However, during the ISF-RF process, the pronounced rough peaks formed by plastic deformation are subjected to extrusion forces from the rolling tool, causing these peaks to be compressed and stacked on the surface, forming material folding traces [50]. In addition to this mechanism, the surface morphology of ISF-RF formed parts under oil lubrication does not show considerable macroscopic interfacial interaction mechanisms. This result is because the oil lubricant is well-retained in the interface and has good heat dissipation properties, reducing the likelihood of adhesion effects, thus leading to improved surface quality of the parts.

By contrast, during ISF-RF under grease lubrication, the poor flowability and heat dissipation of the lubricant result in adhesive effects in some areas under high pressure and poor heat dissipation conditions. These effects cause the surface material of the sheet to be torn, forming unpeeled small flake-like debris during the rotation of the rolling tool, as shown in Fig. 4(b). However, given that grease lubricants have good extreme pressure resistance, the influence of the adhesive effect is relatively minor, resulting in smaller and fewer debris particles, and only a slight decrease in the surface quality of the formed parts. Good surface morphology characteristics have a positive effect on the ISF performance, emphasizing the importance of appropriate lubrication conditions to reduce roughening and adhesive effects, thereby optimizing the surface quality and performance of the formed parts.

As shown in Figs. 4(c) and (d), the surface morphology of ISF-RF formed parts under powder lubrication and dry friction conditions exhibits more pronounced plastic deformation and material accumulation, suggesting a continuous increase in extrusion. The poor adhesion of the powder lubricant to the surfaces of the rolling tool and the sheet metal, combined with the high localized pressure, results in the expulsion of lubricant particles from the deformation zone. This expulsion increases the direct metallic contact area between the tool and sheet. This situation is similar to the contact state under dry friction conditions, where direct tool-sheet contact enhances shear deformation under the direct effect of rolling friction. Additionally, the direct frictional contact increases the likelihood of adhesive effects, resulting in deeper tearing defects compared with those under grease lubrication, and the tearing defects formed under dry friction conditions are more remarkable, accompanied by larger unpeeled flake-like debris. These surface interaction mechanisms contribute to a reduction in forming quality, particularly under dry friction conditions. Poor surface morphology characteristics negatively affect the forming performance, underscoring the detrimental effects of inadequate lubrication on forming quality.

The above analysis reveals that in ISF-RF, the deformation of the surface material under oil and grease lubrication conditions is slightly more pronounced in comparison with ISF-FD. However, adhesive and other interfacial effects are weaker, leading to minimal oxidation of newly exposed Al and Mg on the surface when in contact with air, resulting in only a slight increase in surface oxygen content by 0.54% and 6.45%, respectively (Fig. 6). By contrast, under powder lubrication and dry friction conditions, increased plastic deformation and adhesion expose more exposed Al and Mg on the surface, which react quickly with oxygen in the air, remarkably increasing surface oxygen content by 216.13% and 266.67%, respectively (Fig. 6). The XPS results depicted in Fig. 7(a) also indicate that the oxygen content on the surface of parts under poor lubrication conditions such as dry friction is remarkably higher than under better conditions like oil lubrication. This result validates that under strong rolling friction conditions, the enhanced plastic deformation and adhesion increase the newly exposure of Al and Mg on the surface, which subsequently react with oxygen in the air to form Al_2O_3 and MgO, as evidenced by the spectra shown in Figs. 7(c)-(e). These metal oxides are hard ceramic materials with much higher hardness than their metal counterparts but have lower tensile and flexural strength and are very brittle with poor ductility and toughness. Therefore, the formation of a larger amount of metal oxides on the surface layer is detrimental to the continued plastic deformation of the sheet material, thereby reducing the performance of ISF.

Further analysis reveals that, compared to ISF-FD formed parts subjected only to extrusion deformation, the rolling friction induced additional non-directional shear deformation in the surface layer material, reducing the average grain size of the formed part under oil lubrication by 29.245% (see Fig. 12), along with an increase in the number of intragranular subgrains. Simultaneously, dislocation density increased by 2.871% (see Fig. 13). Additionally, the average Kernel Average Misorientation (KAM) value and High-Angle Grain Boundaries (HAGBs) showed only slight increases of 3.636% and 2.286%, respectively (see Fig. 17). These data indicate that moderate shear deformation induced by rolling friction enhanced deformation stability, effectively suppressing necking and thereby contributing to improved forming performance.

In contrast, under dry friction conditions, the stronger friction effect introduced greater non-directional shear deformation, reducing the average grain size of the formed part by 40.566% (see Fig. 12) and significantly increasing the number of intragranular subgrains. Meanwhile, dislocation density increased by 10.048%, and both the average KAM value and HAGBs significantly rose by 18.182% and 15.429%, respectively (see Fig. 17). These data suggest that intense non-directional shear deformation led to a complex dislocation structure within the surface material, resulting in a marked increase in the average KAM value and elevated local stress levels in the surface material. Furthermore, the notable increase in HAGBs impeded dislocation movement, which, while enhancing surface strength, also elevated local stress, reducing both toughness and ductility and ultimately leading to a decrease in overall forming performance.

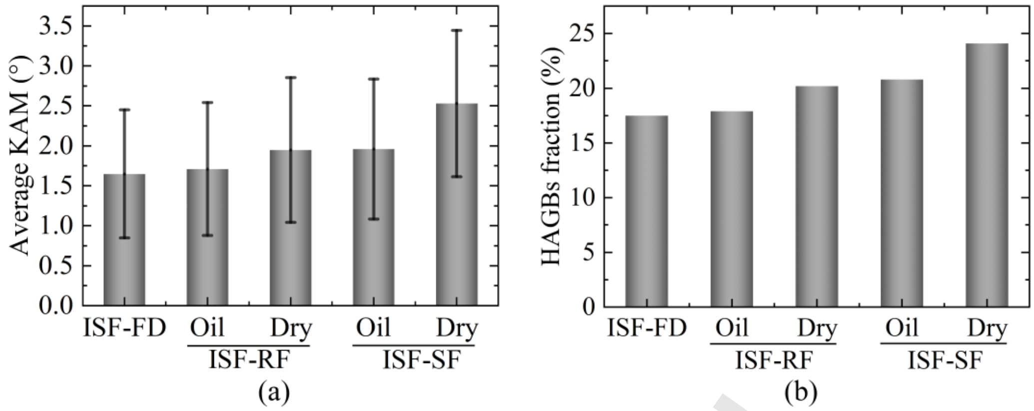

Fig. 17 Orientation analysis of the surface microstructure of incrementally formed parts under different friction modes and lubrication conditions: (a) average kernel average misorientation; (b) high-angle grain boundaries.

During ISF-SF, as shown in Fig. 5, under oil and grease lubrication conditions, the sliding extrusion action drives the surface material to flow along the feed direction. However, some surface material is extruded and bulged, but because its flow rate is much lower than the movement speed of the sliding tool, these materials accumulate on the surface after being extruded, forming material folding. In addition to this phenomenon, the surface shows dense scratches left by the hard asperities of the sliding tool penetrating the surface material of the sheet under high extrusion pressure and high relative sliding speed. The tearing defects on both sides of these scratches are extruded and stacked on the surface, forming material folding traces. Moreover, the higher relative sliding speed exacerbates the expulsion of the lubricant and frictional heat generation, increasing the likelihood of interfacial adhesion effects. Consequently, the internal surface material of the sheet can tear during high relative sliding, resulting in tearing pits and partially unpeeled flake-like debris. Notably, under grease lubrication, the surface morphology also includes microcracks, which may be due to stress concentration caused by high extrusion pressure and uneven strain acting at deeper scratch pit defects, causing them to propagate and form tiny cracks. The interfacial interaction under grease lubrication is intensified, leading to a poorer surface quality compared with oil lubrication.

In ISF-SF under powder lubrication, the high relative sliding speed exacerbates the expulsion of the powder lubricant, leading to poor lubrication effectiveness and remarkably increasing the area of direct contact between the sliding tool and the sheet. This intensifies the shear deformation of the surface material, increases the degree of non-uniform deformation and stress concentration, and results in more pronounced material folding on the surface. Additionally, the direct hard contact during sliding extrusion increases the interfacial adhesion effects and the depth of plowing. Under high relative sliding speeds, this causes tearing deeper within the surface material of the sheet, and coupled with strong shear non-uniform deformation and stress concentration, it can aggravate the propagation of deep surface cracks, even leading to delamination of the surface material and the formation of large flake-like debris. As a result, the surface quality of the formed parts is poor under this lubrication condition, as shown in Fig. 5(c). Under dry friction conditions, direct hard contact further exacerbates the non-uniform shear deformation and stress concentration in the surface material, coupled with interfacial adhesion, plowing, and even localized seizure leading to deeper delamination and the formation of larger block-like debris. The extreme interfacial interaction mechanisms under these conditions result in unacceptable surface quality, as shown in Fig. 5(d). Poor surface morphology significantly reduces the performance of ISF.

Even under the relatively minor sliding friction effects of oil and grease lubrication, the surface material of parts formed by ISF-SF still undergoes a greater degree of plastic deformation compared with those formed by rolling friction. Combined with remarkable plowing and shallow adhesion effects, this exposes more of the underlying material, thereby intensifying the oxidation effect and leading to a notable increase in surface oxygen content by 258.60% and 339.25%, respectively (Fig. 6). Under the conditions of powder lubrication and dry friction, the substantial sliding friction results in even greater plastic deformation of the surface material in sliding friction incremental forming. This, along with the laminar cracking defects, further exposes deeper layers of the sheet material to the air, causing rapid oxidation and showing remarkably higher oxygen content by 1401.08% and 1524.73%, respectively (Fig. 6). The XPS results shown in Fig. 7 further validate this analysis. The spectral analysis of the main elements indicates that the oxidation products are Al_2O_3 and MgO.

When a large amount of Al_2O_3 and MgO is present on the surface of the aluminum alloy sheet, its forming performance is adversely affected in several aspects. Firstly, compared to the base aluminum material, the inherent brittleness and low ductility of Al_2O_3 and MgO significantly reduce the overall ductility and formability of the sheet, hindering continuous plastic deformation. This can lead to premature cracking and failure during the forming process, especially in high-strain areas. Secondly, the hard Al_2O_3 and MgO debris increases abrasive wear at the tool-part interface. This debris may become embedded in the contact surface, increasing friction and tool wear, thereby reducing the surface finish and dimensional accuracy of the formed parts. This also further exacerbates the exposure of internal material on the sheet surface, enhancing the oxidation effect. Thirdly, the interactions such as plowing and adhesion occurring during ISF exacerbate the formation of deep scratches and micro-cracks in the brittle Al_2O_3 and MgO layers. These defects can propagate under continued plastic deformation, increasing the incidence of surface and subsurface cracks, thereby affecting the integrity and mechanical properties of the final product.

Further analysis reveals that sliding friction induces significant additional shear deformation in the feed direction of the surface material, leading to notable changes in grain size, dislocation density, average KAM value, and the number of HAGBs compared to ISF-FD (see Figs. 12, 13 and 17). Under oil lubrication and dry friction conditions, the grain size of ISF-SF parts decreased by 34.34% and 53.46%, respectively, while the dislocation density increased by 7.66% and 26.32%, indicating a substantial increase in the number of subgrains. The average KAM values increased by 18.79% and 53.33%, respectively, and HAGBs fractions increased by 18.86% and 37.71%, correspondingly. These findings indicate that as the sliding friction effect intensifies, the degree of circumferential shear deformation in the material increases significantly.

Similar to ISF-RF, moderate circumferential shear deformation effectively suppresses premature necking, enhancing the formability of the sheet material. However, excessive circumferential shear deformation significantly increases the internal stress level within the surface material and considerably raises dislocation density, leading to complex dislocation pile-ups and further elevating local stress levels. Moreover, the substantial increase in HAGBs notably hinders dislocation motion, preventing the release of localized high stresses, thereby significantly reducing the toughness and ductility of the surface material and negatively impacting its formability.

In summary, regardless of the friction mode, under favorable lubrication conditions (oil and grease lubrication in ISF-RF and oil lubrication in ISF-SF), a moderate increase in non-directional and feed-direction shear deformation contributes to grain refinement, necking suppression, and improved stability in incremental forming [40]. This effect, combined with good surface morphology characteristics mainly resulting from plastic extrusion flow and a relatively low proportion of hard and brittle metal oxides on the surface, leads to a net positive impact on forming performance. This benefit outweighs the slight increase in local stress and reduced ductility caused by dislocation pile-ups. Consequently, the maximum forming angles under oil and grease lubrication in ISF-RF increase by 1.54% and 7.69%, respectively, and under oil lubrication in ISF-SF, the maximum forming angle increases by 10.77%, as shown in Fig. 14(b).

Under grease lubrication in ISF-SF, however, a slight increase in friction effects enhances additional shear deformation in the feed direction and intensifies interfacial mechanisms, somewhat reducing the positive impact of these mechanisms on forming performance while slightly increasing negative effects. In this condition, incremental forming performance is slightly higher than in ISF-FD (increased by 3.08%) but lower than that under oil lubrication (reduced by 7.46%). In contrast, under powder lubrication and dry friction conditions in both friction modes, the excessive additional shear deformation, though it refines the grains, also results in severe local stress concentration within the surface material, significantly reducing toughness and ductility. Strong adhesion and local seizure cause deep tearing, even cracks and layered fractures, with a substantial increase in the proportion of hard and brittle metal oxides on the surface. Combined with these mechanisms, cracks are prone to propagation, leading to a significant decrease in forming performance. Consequently, the maximum forming angle decreases markedly—by 7.69% in ISF-RF and by 23.08% in ISF-SF.

4.3 Friction behavior

In the ISF-FD process, the interface interaction mechanism is illustrated in Fig. 18(a). The target sheet is minimally affected by additional shear deformation caused by friction effects; instead, it primarily experiences localized extrusion deformation associated with the characteristics of ISF. As a result, the overall plastic deformation is limited, with a relatively low density of crystal defects, such as dislocations and subgrains, resulting in a larger grain size in the surface layer. Additionally, due to the deformation characteristics of ISF, the extrusion deformation primarily aligns along the meridional direction of the tool, causing the surface crystal to form a crystallographic texture dominated by planes parallel to {110} (including Brass {110}<112> and {110}<110> orientations). Given the negligible friction effect, the additional shear deformation in the feed direction is minimal, resulting in a negligible twist angle of only 0.309°.

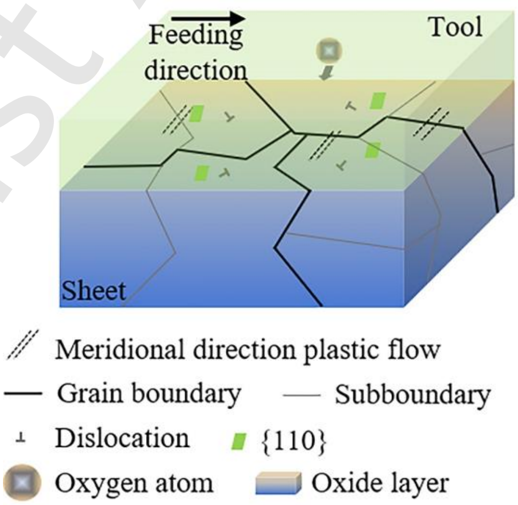

Fig. 18 Mechanism of interface action in near-zero friction incremental sheet forming with free deformation.

Although there are few crystal defects, slight bulges or depressions can still appear at some grain boundaries on the surface, forming mild plastic roughening features. Besides this plastic roughening, other interface mechanisms, such as plowing or adhesion, are absent on the sheet surface, ensuring a high surface quality. Meanwhile, the internal elemental Al and Mg are rarely exposed to the surface, and the oxidation reactions with atmospheric O to form Al_2O_3 and MgO are insignificant. This nearly frictionless incremental forming process is influenced only by extrusion deformation, without other significant interface interaction mechanisms affecting its forming performance. Consequently, the maximum forming angle of the component is moderate, reflecting the inherent forming capabilities of this process.

In ISF-RF process, the surface layer of the sheet material is primarily influenced by two deformation mechanisms, as illustrated in Fig. 19. Firstly, the inherent point-by-point extrusion of ISF induces tensile deformation along the tool's meridional direction, causing the grains to slip in a specific direction and resulting in a {110} crystal plane orientation. Secondly, under the rolling friction mode, the surface layer of the sheet material is subjected to non-directional relative rolling compression with the rolling tool, which generates additional non-directional shear deformation and leaves behind non-directional plastic flow traces on the surface. Consequently, compared to ISF-FD, the overall amount of plastic deformation increases. However, this non-directional deformation characteristic does not lead to specific directional slip of the surface layer crystals, and thus the surface layer crystals of the ISF-RF formed parts still remain parallel to the {110} crystal plane orientation. It is important to note that the additional frictional deformation induced by rolling friction can result in complex slip of the grains, increasing dislocations, sub-grains, and other crystal defects, which slightly enhances the micro-roughness of the surface layer material. Nevertheless, the effective isolation provided by oil and grease lubricants prevents direct hard contact between the sheet and the rolling tool, resulting in no significant macro-interface mechanisms, as shown in Fig. 19(a). Moreover, under interface compressive action, the micro-rough peaks of the surface layer are flattened, leading to a relatively high surface quality and a lower coefficient of friction. It is noteworthy that if the additional frictional deformation caused by rolling friction is not adequately considered, the crystal plane texture orientation induced by extrusion deformation may be misattributed to rolling friction effects, leading to a misunderstanding of the actual friction behavior during ISF-RF process.

Additionally, the oil and grease lubricants provide favorable lubrication conditions, resulting in a relatively low overall degree of plastic deformation of the sheet material, and the interface mechanisms are not significant (compared to powder lubrication and dry friction conditions). Consequently, there are fewer newly exposed, unoxidized aluminum (Al) and magnesium (Mg) elements, and the oxidation effect is also not significant. The limited formation of new metal oxides does not have a substantial impact on the sustained incremental forming performance of the sheet material. Although the non-directional shear deformation introduced by rolling friction is minimal, it still contributes to an increase in the twist angle of the formed parts. This, in conjunction with grain refinement, enhances the stability and performance of the forming process, ultimately leading to an increase in the maximum forming angle.

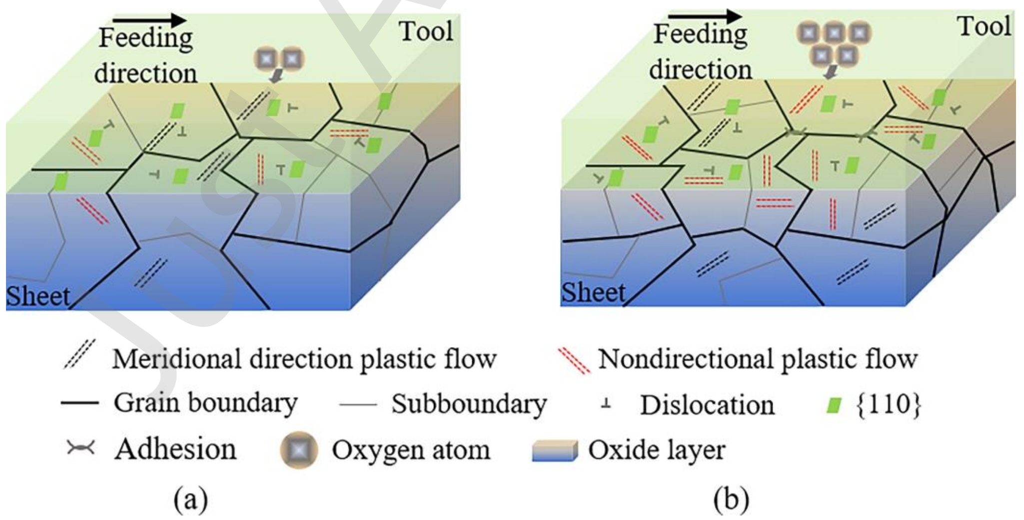

Fig. 19 Mechanism of interface action in incremental sheet forming with rolling friction: (a) oil and grease lubrication conditions; (b) powder lubrication and dry friction conditions.

Under powder lubrication and dry friction conditions, the poor adhesion of the powder lubricant to both the sheet material and the rolling tool results in minimal or even no retained lubricant at the interface. This leads to increased direct hard rolling friction between the rolling tool and the sheet, exacerbating the additional non-directional shear deformation and folding of the surface layer material, as illustrated in Fig. 19(b). Although this induces significant additional rolling friction deformation, its non-directional nature does not alter the {110} crystal plane orientation texture induced by the tensile deformation. This further confirms that observed crystal plane orientations formed by extrusion deformation cannot be regarded as a result of rolling friction behavior when the additional rolling friction deformation is not taken into account.

However, the higher rolling friction deformation complicates the slip of surface layer grains, resulting in a relatively higher dislocation density, an increased number of sub-grains and HAGBs, and a further reduction in grain size, which makes plastic roughening more pronounced. Under direct hard rolling friction conditions, the rough peaks at the interface are more prone to "cold welding" effects without relative sliding, leading to adhesive effects that create tearing defects in the surface layer upon separation. This further degrades surface quality and increases friction coefficient. Given these deformation and interface mechanisms, the original surface material exposed to air reacts with oxygen, generating poorly ductile metal oxides such as Al_2O_3 and MgO, which significantly increases the oxygen content in the surface layer and negatively impacts incremental forming performance.

The strong rolling friction effect introduces more additional rolling friction shear deformation, resulting in an increased twist angle of the formed parts. However, this excessive additional rolling friction deformation significantly increases intra- and inter-grain defects, highlighting localized stress concentrations, which negatively affect forming performance. Combined with the presence of hard and brittle metal oxides and poor surface morphology, these factors exacerbate stress concentration and other interface mechanisms, significantly reducing incremental forming performance and ultimately leading to a decrease in the maximum forming angle of the formed parts.

In ISF-SF process, the surface layer of the sheet material is influenced by two deformation mechanisms, as shown in Fig. 20. First, the inherent point-by-point extrusion of ISF leads to tensile deformation along the tool's meridional direction, resulting in a texture that is parallel to the {110} crystal plane. Second, under the sliding friction mode, the surface layer of the sheet material experiences relative sliding friction along the feed direction between the sliding tool and the material, generating additional oriented shear deformation in the feed direction and leaving behind plastic flow traces along the feed direction on the surface. This friction mode significantly increases the overall plastic deformation of the sheet, which exacerbates as lubrication effectiveness decreases. Simultaneously, the friction deformation characteristics in the feed direction induce specific slip in the surface layer crystals parallel to the {001} plane, forming a {001}<100> cubic texture. Consequently, the surface layer crystals of ISF-SF formed parts exhibit two distinct crystal orientations, namely, parallel to the {110} and {001} crystal planes.

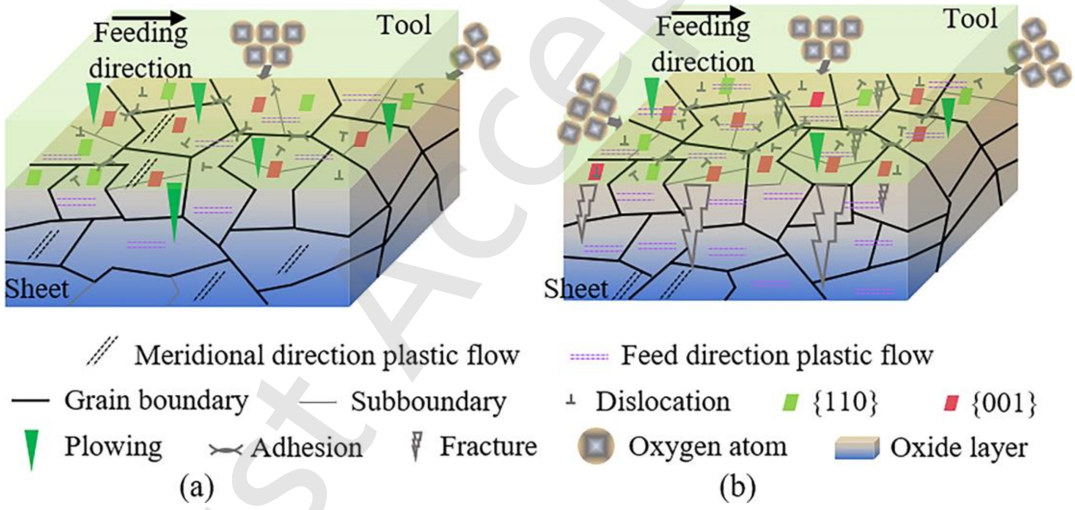

Fig. 20 Mechanism of interface action in incremental sheet forming with sliding friction: (a) oil and grease lubrication conditions; (b) powder lubrication and dry friction conditions.

Under conditions of oil and grease lubrication, the lubricant effectively isolates the sliding tool from the sheet material, minimizing direct hard extrusion sliding friction and thereby resulting in a lower amount of sliding friction deformation. This allows the surface layer crystals to maintain a strong texture aligned with the {110} plane, as illustrated in Fig. 20(a). However, under powder lubrication and dry friction conditions, as lubrication effectiveness declines, the amount of sliding friction deformation increases. The originally unoriented crystals, along with those oriented along the {110} plane due to tensile deformation, tend to slide toward the {001} crystal plane orientation, significantly increasing the amount of crystals oriented along the {001} plane, as shown in Fig. 20(b). Therefore, when sliding friction deformation is not considered, the sliding friction behavior is thought to induce the reorientation of originally unoriented crystal planes toward the {001} and {110} planes. However, considering the additional deformation from sliding friction reveals that the actual sliding friction behavior shifts the {110} crystal plane orientation formed by compressive tensile deformation toward the orientation aligned with the {001} plane due to sliding friction-induced shear deformation.

Additionally, under oil and grease lubrication conditions, the increase in sliding friction deformation in the feed direction adds complexity to the slip systems of the surface layer crystals, leading to dislocation pile-up, lattice distortion, and an increase in subgrains and HAGBs, while reducing grain size. This exacerbates local stress concentrations and further intensifies the degree of plastic roughening. The rough peaks of the sliding tool embed into the surface layer of the sheet under high pressure, creating a plowing effect during relative motion. Additionally, the tiny contact areas between micro-rough peaks are prone to adhesion under high pressure, leading to tearing defects on the surface of the sheet during relative sliding. Particularly under grease lubrication conditions, the shear deformation from sliding friction and stress concentration results in deeper scratches and tearing defects that extend into cracks, further deteriorating surface quality and increasing the friction coefficient.

Thus, even under relatively small sliding friction conditions, the newly exposed internal material significantly increases and reacts with oxygen in the air, producing metal oxides such as Al_2O_3 and MgO, which leads to a notable increase in surface oxygen content. Furthermore, the irregularly shaped hard particles formed from the oxidation of torn debris exacerbate the plowing effect on the surface. The substantial shear deformation introduced by sliding friction along the feed direction significantly increases the twisting angle of the formed parts. Given the above analysis, the beneficial effects of additional sliding friction shear deformation and grain refinement under oil and grease lubrication conditions outweigh the detrimental effects of the hard, brittle metal oxides on the surface layer of the sheet. This results in superior forming performance under oil and grease lubrication compared to conditions without friction. However, excessive through-thickness shear strain under grease lubrication causes the forming performance to be lower than that under oil lubrication.

Under conditions of powder lubrication and dry friction, significant sliding friction shear deformation further increases the complexity of the slip systems in the surface layer crystals. This results in a marked increase in crystal defects and a significant reduction in grain size, while also intensifying stress concentration and the degree of plastic roughening. The increased friction shear deformation in the feed direction causes the twisting angle of the formed parts to rise further. The absence of lubrication exacerbates the direct hard sliding friction contact at the interface between the sheet material and the sliding tool, amplifying the plowing and adhesion effects, and even leading to localized seizing. These effects couple with the shear stresses and uneven plastic flow induced by large sliding friction shear deformation, resulting in plowing scratches and adhesive tearing pits that extend into layered fractures. Consequently, the strong interface mechanisms under these two lubrication conditions lead to extremely poor surface quality and a significantly high friction coefficient.

The large amount of plastic deformation and the strong interface mechanisms further increase the leakage of internal material from the original sheet, exacerbating oxidation effects and producing metal oxides such as Al_2O_3 and MgO, which significantly increase the oxygen content on the surface. These metal oxides, acting as debris, exacerbate surface plowing and crack propagation, and their presence in the surface layer material adversely affects the already poor ductility of the sheet, hindering further plastic deformation. Therefore, the excessive additional sliding friction shear deformation, crystal defects, and strong interface interactions under these two lubrication conditions, in conjunction with the effects of metal oxides, lead to a significant decline in incremental forming performance. Although grain refinement has a positive effect on forming performance, its impact is limited, ultimately resulting in a reduction of the maximum forming angle of the parts.

5 Conclusions

This study systematically investigated the tribological mechanisms governing microstructure evolution in incremental sheet forming (ISF) under rolling friction (ISF-RF), sliding friction (ISF-SF), and near-frictionless deformation (ISF-FD) across lubrication regimes. Key findings revealed distinct friction-mode behaviors:

ISF-RF induced non-directional shear deformation, preserving the extrusion-formed {110} texture while refining grains (>29.245% size reduction) and increasing crystal defects (>2.871%). Optimal lubrication minimized twist angles and suppressed interfacial interactions, whereas poor lubrication amplified adhesion and oxide formation (216.13% increase), highlighting lubrication-dependent microstructural control.

ISF-SF drove directional shear deformation, reorienting texture to {001} and reducing grain size (>34.34%) with elevated defects (>7.66%). Weak friction (e.g., oil lubrication) promoted plowing with minor adhesion, while strong friction (e.g., dry conditions) propagated cracks and fractures via stress concentration and adhesion, exacerbating oxidation and degrading formability (23.08% forming angle reduction).

The study revealed that under weak friction effects, both rolling and sliding friction modes (ISF-RF/ISF-SF) generated moderate shear deformation, refining grain structures and enhancing formability beyond the adverse interfacial interactions, thereby outperforming near-frictionless forming (ISF-FD). In contrast, strong friction effects induced excessive shear deformation, which significantly increased surface crystal defect density. Coupled with stress concentration and metal oxide accumulation, this reduced surface ductility, promoted crack propagation and delamination fractures, and led to substantial performance degradation.

By establishing a microstructure-property-process relationship, this study provides a theoretical foundation for optimizing ISF through adaptive lubrication strategies and selective friction mode utilization: ISF-RF for texture preservation and ISF-SF for controlled grain refinement. These insights advance high-precision forming technologies by offering a scientific framework for industrial ISF optimization, emphasizing defect suppression, oxidation management, and friction-mode selection to harmonize microstructural benefits with interfacial stability.

Acknowledgements

The authors gratefully acknowledge support from the National Key R&D Program of China (Grant No. 2023YFB3407003), the National Natural Science Foundation of China (Grant No. 52375378), the Shaanxi Province Science Fund for Distinguished Young Scholars (Grant No. 2025JC-JCQN-021), and the Shaanxi Province Natural Science Foundation - Young Scientists Project (Grant No. 2025JC-YBQN-701).

Declaration of competing interest

The authors have no competing interests to declare that are relevant to the content of this article.

References

[1] Tian C, Zhang D W, Yang G C, Zhu C C, Zhao S D. A new forming limit test method for incremental stretch flanging. Journal of Materials Processing Technology 319: 118082 (2023)

[2] Liu F Y, Li Y L, Yuan H, Sun R W, Li F Y, Li J F. Comprehensive modeling of forming forces in three directions for incremental sheet forming process based on the contact area. Journal of Manufacturing Processes 84: 986-1000 (2022)

[3] Behera A K, De Sousa R A, Ingarao G, Valentin O. Single point incremental forming: An assessment of the progress and technology trends from 2005 to 2015. Journal of Manufacturing Processes 27: 37-62 (2017)

[4] Chang Z D, Li M, Chen J. Analytical modeling and experimental validation of the forming force in several typical incremental sheet forming processes. International Journal of Machine Tools and Manufacture 140: 62-76 (2019)

[5] Thanh Vu N, Tuyen V, Nhat Tuan P, Le Cao Ky D. Reviews on the Effect of Single Point Incremental Forming (SPIF) Process Parameters on Surface Roughness of Aluminum Alloy AA1050-H14 Sheet Metal. Applied Mechanics and Materials 914: 151-162 (2023)

[6] Pratheesh Kumar S, Elangovan S, Mohanraj R, Boopathi S. A comprehensive review in incremental forming on approaches of deformation analysis and surface morphologies. Materials Today: Proceedings 43: 3129-3139 (2021)

[7] Zhu H, Ou H G. A new analytical model for force prediction in incremental sheet forming. Journal of Materials Processing Technology 318: 118037 (2023)

[8] Viet M V, Thinh N T, Sy L V. Effect of Lubrication on Deforming the Aluminum Sheet with Two Points Incremental Forming Technology. In: Proceedings of the 2nd Annual International Conference on Material, Machines and Methods for Sustainable Development, Nha Trang, Vietnam, 2001: 975-982.

[9] Xu D K, Wu W C, Malhotra R, Chen J, Lu B, Cao J. Mechanism investigation for the influence of tool rotation and laser surface texturing (LST) on formability in single point incremental forming. International Journal of Machine Tools & Manufacture 73: 37-46 (2013)

[10] Strano M, Sorrentino L, Carrino L. Some issues about tools and friction in the negative dieless incremental forming process. In: Proceedings of the 10th Metal Forming. Krakow, Poland, 2004: 345-349.

[11] Jeswiet J, Micari F, Hirt G, Bramley A, Duflou J, Allwood J. Asymmetric Single Point Incremental Forming of Sheet Metal. CIRP Annals 54(2): 88-114 (2005)

[12] Kim Y H, Park J J. Effect of process parameters on formability in incremental forming of sheet metal. Journal of Materials Processing Technology 130-131: 42-46 (2002)

[13] Silva M B, Bay N, Martins P A F. Hole-Flanging by Single Point Incremental Forming, in: Davim JP (Eds.), Materials Forming and Machining, Elsevier. Ltd, 2016, pp. 25-50.

[14] Eyckens P, Van Bael A, Van Houtte P. Marciniak–Kuczynski type modelling of the effect of through-thickness shear on the forming limits of sheet metal. International Journal of Plasticity 25(12): 2249-2268 (2009)

[15] Allwood J M, Shouler D R. Generalised forming limit diagrams showing increased forming limits with non-planar stress states. International Journal of Plasticity 25(7): 1207-1230 (2009)

[16] Emmens W C, van den Boogaard A H. An overview of stabilizing deformation mechanisms in incremental sheet forming. Journal of Materials Processing Technology 209(8): 3688-3695 (2009)

[17] Malhotra R, Xue L, Belytschko T, Cao J. Mechanics of fracture in single point incremental forming. Journal of Materials Processing Technology 212(7): 1573-1590 (2012)

[18] Xu D K, Malhotra R, Chen J, Lu B, Cao J. Numerical and experimental studies for the effects of through-the-thickness shear on formability in single point incremental forming. AIP Conf. Proc 1532: 969-976 (2013)

[19] Yang Z Y, Chen F. Mechanism of twist in incremental sheet forming of thermoplastic polymer. Materials & Design 195: 108997 (2020)

[20] Chang Z D, Chen J. Mechanism of the twisting in incremental sheet forming process. Journal of Materials Processing Technology 276: 116396 (2020)

[21] Carrino L, Di N M, Sorrentino L, Strano M. The influence of friction in the negative dieless incremental forming process. In: Proceedings of the 9th International ESAFORM Conference on Material Forming, Glasgow, Britain, 2006: 207-210.

[22] Durante M, Formisano A, Langella A. Observations on the Influence of Tool-Sheet Contact Conditions on an Incremental Forming Process. Journal of Materials Engineering and Performance 2011;20(6):941-946. https://doi.org/10.1007/s11665-010-9742-x

[23] Duflou J R, Callebaut B, Verbert J, De Baerdemaeker H. Laser assisted incremental forming: formability and accuracy improvement. CIRP Ann Manuf Technol 56(1): 273–276 (2007)

[24] Bobzin K, Bagcivan N, Ewering M, Warnke C. Investigations on Nanolaminated TiZrN/CrN as a Tribological PVD Hard Coating for Incremental Sheet Forming Tools. Advanced Engineering Materials 11(8): 674-679 (2009)

[25] Wei H, Hussain G, Iqbal A, Zhang Z P. Surface roughness as the function of friction indicator and an important parameters-combination having controlling influence on the roughness: recent results in incremental forming. Int J Adv Manuf Technol 101(9-12): 2533-2545 (2018)

[26] Esmaeilpour R, Kim H, Park T, Pourboghrat F, Agha A, Abu-Farha F. Effect of hardening law and process parameters on finite element simulation of single point incremental forming (SPIF) of 7075 aluminum alloy sheet. Mech Ind 21(3): 302 (2020)

[27] Duflou J R, Habraken A M, Cao J, Malhotra R, Bambach M, Adams D, et al. Single point incremental forming: state-of-the-art and prospects. International Journal of Material Forming 11(6): 743-773 (2017)

[28] Azevedo N G, Farias J S, Bastos R P, Teixeira P, Davim J P, Alves de Sousa R J. Lubrication aspects during single point incremental forming for steel and aluminum materials. Int J Precis Eng Manuf 16(3): 589–595 (2015)

[29] Li Z F, Lu S H, Zhang T, Mao Z X, Zhang C. A Simple and Low-Cost Lubrication Method for Improvement in the Surface Quality of Incremental Sheet Metal Forming. Transactions of the Indian Institute of Metals 71(7): 1715-1719 (2018)

[30] Xu Z Y, Xu Y, Hu K H, Xu Y F, Hu X G. Formation and tribological properties of hollow sphere-like nano-MoS2 precipitated in TiO2 particles. Tribology International 81: 139-148 (2015)

[31] Diabb J, Rodríguez C A, Mamidi N, Sandoval J A, Taha-Tijerina J, Martínez-Romero O, et al. Study of lubrication and wear in single point incremental sheet forming (SPIF) process using vegetable oil nanolubricants. Wear 376(part A): 777-785 (2017)

[32] Şen N, Şirin Ş, Kıvak T, Civek T, Seçgin Ö. A new lubrication approach in the SPIF process: evaluation of the applicability and tribological performance of MQL. Tribol Int 171: 107546 (2022)

[33] Torres H, Vuchkov T, Slawik S, Gachot C, Prakash B, Rodríguez Ripoll M. Self-lubricating laser claddings for reducing friction and wear from room temperature to 600 °C. Wear 408-409: 22–33 (2018)

[34] Hussain G, Gao L, Hayat N, Cui Z, Pang YC, Dar N U. Tool and lubrication for negative incremental forming of a commercially pure titanium sheet. J Mater Process Technol 203(1–3): 193–201 (2008)

[35] Rodriguez-Alabanda O, Guerrero-Vaca G. Influence of single point incremental forming on the quality and surface properties of parts manufactured with aluminized steel sheets pre-coated with PTFE. CIRP Journal of Manufacturing Science and Technology 38: 215-229 (2022)

[36] Zhang Q, Xiao F, Guo H, Li C, Gao L, Guo X, et al. Warm negative incremental forming of magnesium alloy AZ31 sheet: new lubricating method. J Mater Process Technol 210(2): 323-329 (2010)

[37] Hussain G, Al-Ghamdi K A. PEO coating as lubrication means for SPIF of titanium sheet: characteristics and performance. Mater Res Innov 18(sup2): S2-727-S2-733 (2014)

[38] Astarita A, Carrino L, Durante M, Formisano A, Langella A, Minutolo F M C, et al. Experimental study on the incremental forming of coated aluminum alloy sheets. Key Eng Mater 622-623: 398-405 (2014)

[39] Kilani L, Mabrouki T, Ayadi M, Chermiti H, Belhadi S. Effects of rolling ball tool parameters on roughness, sheet thinning, and forming force generated during SPIF process. International Journal of Advanced Manufacturing Technology 106(9-10): 4123-4142 (2020)

[40] Lu B, Fang Y, Xu D K, Chen J, Ou H, Moser N H, et al. Mechanism investigation of friction-related effects in single point incremental forming using a developed oblique roller-ball tool. Int J Mach Tools Manuf 85: 14–29 (2014)

[41] Fan G Q, Gao L, Li W J, Sun F T. A Study of the Friction and Lubrication in Electric Hot Incremental Forming of TC4 Sheet. Mechanical Science and Technology 29(2): 201-205 (2010) (in Chinese)

[42] Silva G C, Souza L M R, Patrício L F S. Evaluation of surface roughness in the incremental forming process with variation in the degrees of freedom of the contact tool. Journal of the Brazilian Society of Mechanical Sciences and Engineering 44: 168 (2022)

[43] Naranjo J A, Miguel V, Coello J, Manjabacas M C, Martinez-Martinez A, Garcia-Martinez E. Tribological Characterization of the Heat-Assisted Single Point Incremental Forming Process Applied to the Ti6Al4V Alloy with the Definition of an Adhesion Parameter for the Tool Surface. Materials 14(24): 7641 (2021)

[44] Sabet A S, Domitner J, Ristić A, Öksüz K I, Ripoll M R, Sommitsch C. Effects of temperature on friction and degradation of dry film lubricants during sliding against aluminum alloy sheets. Tribology International 180: 108205 (2023)

[45] Mekicha M A, de Rooij M B, Mishra T, Matthews D T A, Jacobs L, Schipper D J. Study of wear particles formation at single asperity contact: An experimental and numerical approach. Wear 470-471: 203644 (2021)

[46] Zhang D W, Yang G C, Zhao S D. Frictional behavior during cold ring compression process of aluminum alloy 5052. Chinese Journal of Aeronautics 34(5): 47-64 (2021)

[47] Nian J Y, Si Y F, Guo Z G. Advances in atomic-scale tribological mechanisms of solid interfaces. Tribology International 94: 1-13 (2016)

[48] Vorholt J, Shimizu T, Kobayashi H, Heinrich L, Flosky H, Vollertsen F, et al. In-situ observation of lubricant flow on laser textured die surface in sheet metal forming. Procedia Engineering 207: 2209-2214 (2017)Author biography

[49] Singh R P, Kumar S, Pande S, Salunkhe S, Ragab A E, Singh P K, et al. Robot-Assisted Cold and Warm Incremental Sheet Forming of Aluminum Alloy 6061: A Comparative Study. Metals 13(3): 568 (2023)

[50] Yang G C, Zhang D W, Tian C, Hu Y H, Zhao S D. A method for determining efficiency parameters based on efficiency-quality graph in incremental sheet forming. Journal of Materials Research and Technology 33: 5170-5192 (2024)

[51] Yang G C, Zhang D W, Tian C, Zhao S D. A new test for friction in incremental sheet forming: method and implementation. Transactions of Nonferrous Metals Society of China 2024. (in press)

Guangcan YANG. She is a Ph.D. student at the School of Mechanical Engineering, Xi'an Jiaotong University, China. Her research primarily investigates the friction characteristics and interfacial behaviors in incremental sheet forming processes. She has developed a new friction test method tailored for tribological analysis in incremental sheet forming.

Da-Wei ZHANG. He is a professor at School of Mechanical Engineering, Xi’an Jiaotong University, China. He received his Ph.D. degree in 2012 from Northwestern Polytechnical University, Xi’an, China. His research interests include material forming technology and equipment, hydraulic system, tribology, etc.

Chong TIAN. He is a PH.D. student from School of Mechanical Engineering, Xi'an Jiaotong University, China. Engaged in incremental forming research, focusing on the forming limit of the incremental forming process, the incremental forming technology and equipment in the sheet/tube flanging process, etc.

Sheng-Dun ZHAO. He received his MS and Ph.D. degrees in mechanical engineering from School of Mechanical Engineering, Xi’an Jiaotong University, China, in 1986 and 1997, respectively. His current position is a professor at School of Mechanical Engineering, Xi’an Jiaotong University, China. His research areas cover the plastic forming technology and equipment, computer control of mechanical electrical-hydraulic system, and fluid transmission and control, etc.